The putative influence of the agr operon upon survival mechanisms used by Clostridium acetobutylicum

Jabbari, Sara; Steiner, Elisabeth; Heap, John T; Winzer, Klaus; Minton, Nigel P; King, John R

DOI:
10.1016/j.mbs.2013.03.005

Document Version
Peer reviewed version

Citation for published version (Harvard):
Jabbari, S, Steiner, E, Heap, JT, Winzer, K, Minton, NP & King, JR 2013, 'The putative influence of the agr operon upon survival mechanisms used by *Clostridium acetobutylicum*', *Mathematical biosciences*, vol. 243, no. 2, pp. 223-39. https://doi.org/10.1016/j.mbs.2013.03.005

The putative influence of the *agr* operon upon survival mechanisms used by *Clostridium acetobutylicum*

Sara Jabbari[a,*], Elisabeth Steiner[b], John T. Heap[c], Klaus Winzer[b], Nigel P. Minton[b], John R. King[d]

[a] *School of Mathematics and Centre for Systems Biology, University of Birmingham, Edgbaston Campus, Birmingham, B15 2TT, UK*
[b] *BBSRC Sustainable Bioenergy Centre, School of Molecular Medical Sciences, Centre for Biomolecular Sciences, University of Nottingham, Nottingham, NG7 2RD, UK*
[c] *Centre for Synthetic Biology and Innovation, Division of Molecular Biosciences, Imperial College London, South Kensington Campus, London, SW7 2AZ, UK*
[d] *Centre for Mathematical Medicine and Biology, School of Mathematical Sciences, University of Nottingham, Nottingham, NG7 2RD, UK*

Abstract

The bacterium *Clostridium acetobutylicum* produces acids as an energy-yielding process during exponential growth. An acidic environment, however, is toxic to the cells and two survival mechanisms are in place to prevent them from dying. Firstly, during a solventogenesis phase, the cells take up these acids and convert them to solvents, thus raising the environmental pH. Secondly, the cells undergo sporulation to form highly resistant spores capable of surviving extreme conditions. One possible regulatory mechanism for these processes is the accessory gene regulatory (*agr*) quorum-sensing system, which is thought to coordinate cell population density with cell phenotype. We model this system to monitor its putative effect upon solventogenesis and the sporulation-initiation network responsible for triggering spore formation. We demonstrate that a high population density should be able to induce both solventogenesis and sporulation, with variations to the parameter set allowing sporulation alone to be triggered; additional distinct signals are capable of restoring the solventogenic response. We compare the *agr* system of *C. acetobutylicum* with that of *Staphylococcus aureus* in order to investigate why the differences in feedback between the two systems may have evolved. Our findings indicate that, depending upon the mechanism of interaction between the *agr* system and the sporulation-initiation network, the clostridial *agr* circuitry may be in place either to moderate the number of spores that are formed (in order for this number to reflect the urgency of the situation), or simply as an energy-saving strategy.

Keywords: Clostridium acetobutylicum, Gene regulation networks, Mathematical modelling, Quorum sensing, Solventogenesis, Sporulation

*Corresponding author
Email addresses: sara.jabbari@nottingham.ac.uk (Sara Jabbari), e.steiner@aon.at (Elisabeth Steiner), j.heap@imperial.ac.uk (John T. Heap), klaus.winzer@nottingham.ac.uk (Klaus Winzer), nigel.minton@nottingham.ac.uk (Nigel P. Minton), john.king@nottingham.ac.uk (John R. King)

1. Introduction

Clostridium acetobutylicum is an anaerobic endospore-forming Gram-positive bacterium. While many clostridial species, for example *Clostridium difficile*, are well known for their pathogenicity, *C. acetobutylicum* is non-virulent and, instead, is best known for its ability to produce butanol. When grown in batch culture, *C. acetobutylicum* will initially produce the acids acetate, butyrate and lactate. During the transition to stationary phase, when growth ceases, the cells switch from the production of acids to solvents, namely acetone, butanol and ethanol. The latter process is often referred to as acetone-butanol, or AB, fermentation. For a detailed review of AB fermentation see [1].

The fermentation process is energy-yielding (generating ATP) and the acids and solvents are simply by- or waste-products of the various reduction and oxidation reactions that take place. However, these so-called waste products have motivated much of the research into this bacterium as supplies of butanol, which has properties making it suitable as an alternative fuel source to petrol, are much sought-after. Thus, given the current concerns over fossil fuels, a great deal of research is focused upon maximising clostridial butanol production, either through genetic manipulation or through the signals which trigger solventogenesis.

For butanol production to be enhanced, the mechanisms governing the onset of solventogenesis must be well understood. At present it is postulated that the switch to solvent production occurs as a survival mechanism: acid production lowers the pH of the environment making it a less favourable habitat for the bacteria (the toxicity of undissociated acetate and butyrate causes cell death); solventogenesis involves the uptake of these acids, thus simultaneously raising the environmental and cellular pH and acting as a defence mechanism against the acidic conditions [1].

The onset of solventogenesis is also believed to be linked, possibly indirectly, to sporulation, since the two occur at similar states of cell growth; see [2] for example. Sporulation is a complex developmental process that enables bacteria to form dormant, extremely resilient spores as an alternative survival strategy to competing for nutrients through rapid vegetative growth. A spore is formed through asymmetric division of a vegetative cell (vegetative growth requires symmetric division), resulting in a mother cell and a forespore. The latter is engulfed by the mother cell, which manufactures a highly resistant coating around the newly formed spore cell (which is resistant to extreme conditions such as a lack of nutrients or extreme pH) before dying; see for example [3, 4, 5, 6].

The model organism for sporulation in Gram-positive bacteria is *Bacillus subtilis* with the master regulator responsible for inducing the genes required for the actual process of sporulation

being Spo0A (which is phosphorylated in its active form) [7]. The gene regulation network that detects sporulation-conducive conditions and either activates or suppresses Spo0A (as appropriate according to the conditions) is well-defined in *B. subtilis* [8, 9, 10] and, while some distinctions exist (most notably the absence of a nutrient-starvation trigger in *C. acetobutylicum*), there is a great deal of overlap between this network and what is known of the corresponding one in *C. acetobutylicum* [8, 11] (and indeed in other clostridial species), allowing us to draw on previous modelling work of *B. subtilis* [9] to create a suitable model for *C. acetobutylicum*. Furthermore, transcription of certain of the enzymes governing solventogenesis is under the control of Spo0A: putative binding sites have been identified in the region of their transcription start sites [12, 13]. Thus we can add a downstream module to the model covering Spo0A-induced solvent production.

The *agr* quorum-sensing system has recently been shown to form part of the regulation of sporulation in *C. acetobutylicum* [14]. Quorum sensing is a cell signalling mechanism whereby individual cells secrete signal molecules into the external environment. The cells can detect these molecules and adapt their behaviour according to an estimated population density. An acidic environment is most likely to occur either when the population of cells is large or when diffusion is limited, both being circumstances under which a quorum-sensing system is triggered. This may therefore be an effective way of detecting when a toxic environment may occur: instead of waiting until the environment reaches a threshold toxic level, quorum sensing can help forewarn when this will occur, thus allowing the cells to act before such conditions have been reached. Interestingly, it was shown that the *agr* system has no noticeable effect upon solventogenesis in *C. acetobutylicum*, despite both sporulation and solventogenesis being assumed to be related survival mechanisms. This thus raised questions about the point of entry of the *agr* response regulator into the gene regulation networks governing the initiation of these survival mechanisms. If it enters upstream of Spo0A, should both phenotypes not be induced? We investigate this from a computational perspective.

We formulate a model incorporating a sporulation-initiation network, the *agr* quorum-sensing system and acid and solvent production, demonstrating that a high population density could, in theory, induce both solventogenesis and sporulation if the *agr* proteins lie upstream of Spo0A in the overall network. Variations to the parameter set allow sporulation to be triggered, with cells still remaining in acidogenic phase; additional signals are capable of restoring the solventogenic response. The converse was not possible, matching the experimental results of [14], while demonstrating that the *agr* system could still be involved in solventogenesis in other clostridial bacteria.

The *agr* operon consists of four genes, two of which code for the propeptide precursor (the quorum-sensing signal-molecule) and its processing enzyme with the remaining two responsible for

signal detection and eliciting a response (informed via a two-component system). In *S. aureus*, all four genes are subject to increased transcription as a result of high population density [15]. Previous modelling studies have suggested that feedback into the two-component system is the key to a fully effective quorum-sensing system [16], but, interestingly, these two feedback loops appear to be absent in *C. acetobutylicum* [17]. Comparisons with the staphylococcal *agr* system indicate that, depending upon the mechanism of interaction between the *agr* system and the sporulation-initiation network, the clostridial *agr* circuitry may (at least in part) be in place either to moderate the number of spores that are formed (in order for this number to reflect the urgency of the situation), or simply as an energy-saving strategy.

2. Model formulation

2.1. Preliminaries

Existing models of the *agr* operon relate to this quorum-sensing system in *S. aureus* and its effect upon virulence-factor production [16, 18, 19]; to our knowledge no models of the *agr* operon exist in the context of the clostridial species. In a similar vein, models of sporulation in Gram-positive bacteria predominantly concern *B. subtilis*, with three in particular incorporating genetic regulation of the initiation network [9, 20, 21] using methods similar to those that we shall exploit here. Mathematical modelling of *C. acetobutylicum* has concentrated on the metabolic interactions involved in the fermentation process and have successfully represented the cells either during acidogenesis or in solventogenesis [22, 23, 24, 25, 26]. However, the nature of the existing models means that the switch between the two phases has to be imposed either by an artificial switch, or by an alteration in the parameter set. Instead of creating a metabolic model of the fermentation process, we seek here to model the regulatory proteins that are controlled by signals within the environment of the cells, namely the population density and the environmental pH. These proteins can then determine the phenotype of the cells, in terms both of the fermentation process (acid or solvent production) and of cell type (vegetative or spore). We model a population of *C. acetobutylicum* in batch culture whereby the cells grow in a closed environment in which signal molecules can accumulate and trigger a quorum-sensing-related response. The model can be divided into three modules:

- the cells' phenotype, i.e. vegetative or spore cell, acid or solvent phase;
- the sporulation-initiation network (excluding the *agr* operon);
- the *agr* operon.

We accordingly split our discussion of the model formulation into these three components.

Variable	Concentration
H	extracellular acids
S_v	extracellular solvents
N_v	vegetative cells
N_s	spores
K	Kin
K^P	Kin∼P
P_h	Pho
P_h^P	Pho∼P
S_A	Spo0A
S_A^P	Spo0A∼P
A_b	AbrB tetramer
σ^H	sigma factor, σ^H
A	AgrA
A^P	AgrA∼P
B	intracellular AgrB/D
C	intracellular AgrC
R	transmembrane AgrC (receptor)
S	transmembrane AgrD (signal precursor)
T	transmembrane AgrB
a	free AIP
R^P	AIP-bound phosphorylated transmembrane AgrC

Table 1: Definitions of the variables. The table is divided into sections corresponding to the modules of the model. We note that, after [16], intracellular AgrB and AgrD are assumed to be present in equal quantities.

Parameter	Rate of
c_X	production of species X (a protein when its gene has only one promoter)
c_X^i	production of protein X directed by promoter i
	(where its gene has multiple promoters)
c_X^{il}	production of protein X directed by promoter i at some specified lower rate
c_X^{ih}	production of protein X directed by promoter i at some specified higher rate
c_{agr}^l	basal production of intracellular AgrB and AgrD
c_{agr}^h	AIP-induced production of intracellular AgrB and AgrD
c_{agr}^{CA}	constitutive production of AgrA and AgrC
B_X^Y	binding of the regulatory molecule X to a promoter site
	of the gene encoding for Y
U_X^Y	unbinding of the regulatory molecule X from a promoter site
	of the gene encoding for Y
$B_{A^P}^{agr}$	binding of AgrA∼P to the promoter site of the *agr* operon
$U_{A^P}^{agr}$	unbinding of AgrA∼P from the promoter site of the *agr* operon
β_{R^P}	binding of AIP to transmembrane AgrC
γ_{R^P}	spontaneous separation of AIP from transmembrane AgrC
λ_X	degradation of X
α	autophosphorylation of Kin
ϕ_X^Y	phosphotransfer from molecule X to molecule Y
ψ_X	spontaneous dephosphorylation of X
δ_H	acid-induced cell death
δ_{S_v}	solvent-induced cell death
δ_H^a	acid-induced AIP degradation
$\delta_{S_v}^a$	solvent-induced AIP degradation
ξ	spore formation
μ_{agr}	intracellular Agr proteins take up into the cell membrane
k_{agr}	AIP production
μ_e	acid/solvent secretion
μ_i	acid/solvent internalisation
ρ	acid conversion into solvent
r	vegetative cell growth
κ	vegetative cell carrying capacity

Table 2: Definitions of the parameters. Units are given in Table 3 with the default parameter values.

2.2. Cell phenotype

The first module of the model concerns cell phenotype, i.e. the concentrations of vegetative cells, spores, acids (acetate, butyrate and lactate) and solvents (acetone, butanol and ethanol). We model vegetative cell growth as logistic (as is appropriate for cells grown in batch culture) and assume that they are killed at a rate δ_H by acids and δ_{S_v} by solvents. Spo0A is required for both sporulation and solventogenesis [13] and we assume that it must be activated, i.e. phosphorylated, to induce either of these responses. For simplicity, we assume this relationship to be linear so that spore formation occurs at rate ξ times the concentration of Spo0A∼P in a vegetative cell (S_A^P), see Tables 1 and 2 for definitions of the variables and parameters, though in reality it is possible that this relationship would be nonlinear so that sporulation occurs only above a threshold Spo0A∼P level. Acids are produced constitutively at rate c_H before diffusing across the cell membrane at rates μ_e (externalisation) and μ_i (internalisation). Acid conversion into solvents occurs at rate ρ times S_A^P. Fully formed spores no longer produce acids or solvents. Thus the equations representing cell phenotype are given by

$$\frac{dN_v}{dt} = rN_v\left(1 - \frac{N_v}{\kappa}\right) - (\delta_H H + \delta_{S_v} S_v)N_v - \xi S_A^P N_v, \tag{1}$$

$$\frac{dN_s}{dt} = \xi S_A^P N_v, \tag{2}$$

$$\frac{dH}{dt} = \frac{\mu_e}{(\mu_e + \mu_i)}\left(c_H N_v - \frac{\mu_i \rho}{\mu_e} S_A^P H\right), \tag{3}$$

$$\frac{dS_v}{dt} = \frac{\mu_i}{(\mu_e + \mu_i)} \rho S_A^P H. \tag{4}$$

Strictly speaking, N_v encapsulates both vegetative cells and cells that have embarked upon, but not yet completed, the sporulation process, but we refer to this variable simply as the number of vegetative cells. The full four equations representing internal and external concentrations of acids and solvents are simplified through the assumption that externalisation and internalisation of these products are fast in relation to acid production and conversion; this yields (3) and (4).

Experimental data used to generate wild-type results for [14] were used to fit specific parameters and conditions. Because the methods used do not calculate vegetative and spore cells directly, some data conversion was required to make them suitable for use with this model. OD_{600} measurements were scaled so that the maximum total cell count was 5×10^8. Assuming the final OD_{600} measurement accounted solely for spores, the heat-resistant colony forming unit (cfu) data were scaled so that the final cfu count matched that of the final scaled OD_{600} data point, yielding an approximation of the spore count. Finally, subtraction of the spore count from the scaled OD_{600} data generated an estimate of the vegetative cell level. From the resulting data (which will be depicted in Figure 4, we obtain the initial conditions $N_v(0) = 8.1 \times 10^6$ cells ml^{-1}, $N_s(0) = 0$ cells ml^{-1} (i.e. initially all cells are vegetative), $H = 0.16$ mM and $S_v = 1$ mM.

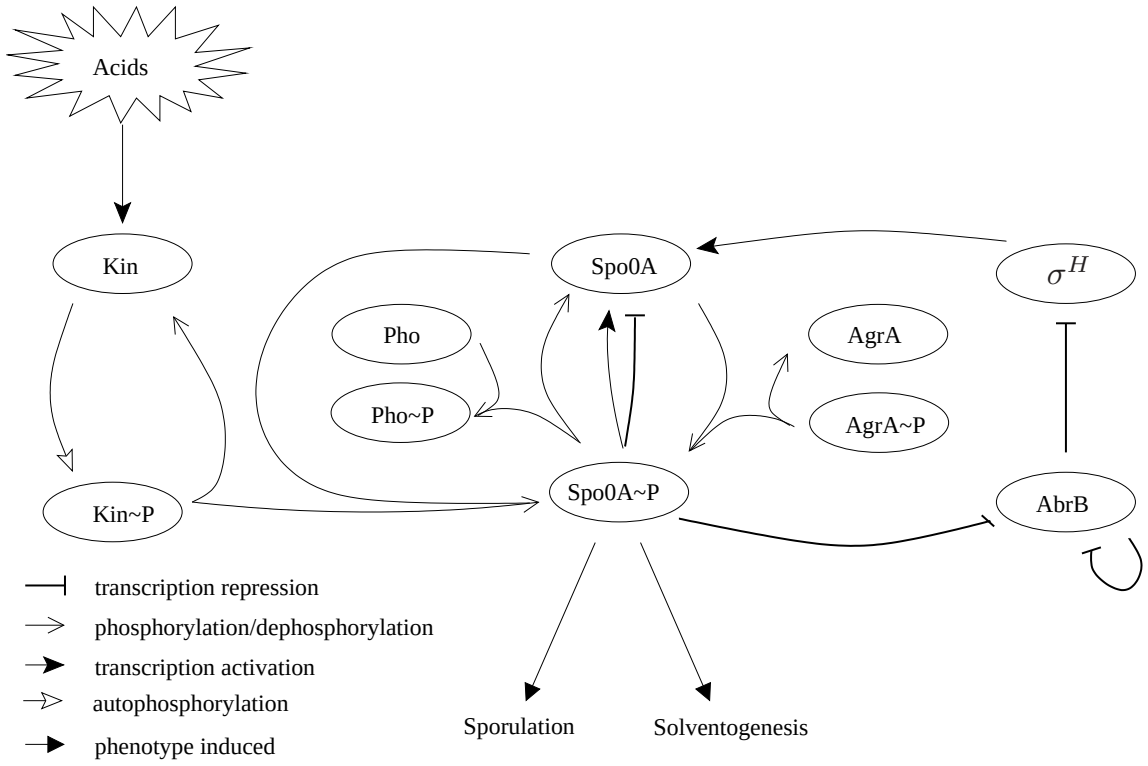

Figure 1: A schematic representation of the network governing sporulation-initiation in *C. acetobutylicum*. We include a putative kinase (Kin) which may be transcribed in response to a sporulation-positive signal and a phosphatase (Pho) which acts upon Spo0A. This kinase autophosphorylates and transfers its phosphate to Spo0A. Increased levels of phosphorylated Spo0A both activate a solventogenesis and sporulation response and inhibit transcription of AbrB, a transition state regulator. Notice that we have assumed Spo0A to self-regulate in the same manner as in *B. subtilis*: Spo0A∼P inhibits low-level transcription of *spo0A* while activating high-level transcription; see [9] for more details. We demonstrate, in this figure, one possible interaction between AgrA∼P and the sporulation-initiation network, i.e. via direct phosphorylation of Spo0A. In Figure 2 we illustrate alternative possibilities.

2.3. The sporulation-initiation network

Figure 1, guided by the literature, illustrates the most likely components of the network governing sporulation-initiation in *C. acetobutylicum*, the second module of the model. Comparison with Figure 2 of [9] reveals the overlap between the two, namely the proteins Spo0A (the response regulator of the system), AbrB (a sporulation repressor and global transcription regulator) and the sigma factor σ^H (sigma factors are subunits of bacterial polymerase which attach to the core polymerase in effect responsible for recognising the promoter sequence on DNA and initiating transcription). A SinR homologue (though, interestingly not SinI) has been identified in *C. acetobutylicum* [27] but, contrary to *B. subtilis*, there is no evidence that it affects Spo0A or Spo0A∼P levels. It is accordingly omitted from this model. Assuming that Spo0A, AbrB and σ^H interact in the same

manner as in *B. subtilis*, we can extract the relevant equations directly from [9]. In the clostridial species kinases are capable of directly phosphorylating Spo0A [28]. We include a kinase which we call simply Kin in the model. We assume that transcription of the kinase increases in accordance with acid levels (this would be mediated by a signalling mechanism not included in the model) and, guided by [29], we assume that this protein autophosphorylates upon translation, transferring the phosphate directly to Spo0A (as might occur if the cells are in an environment conducive to sporulation). The presence of a kinase is generally accompanied with that of a phosphatase acting upon the same target protein (evidence of this is seen in [28]) and we accordingly include this in the model (labelled Pho in Figure 1). In §3 we investigate whether or not the kinase is required, or indeed sufficient, for the model to display the behaviour observed experimentally.

Conventional reaction kinetics are used to construct the equations (further details can be found in [9]). The equations representing the sporulation-initiation network are given by

$$\frac{dS_A}{dt} = \frac{c^1_{S_A} U^{S_A}_{S^P_A}}{B^{S_A}_{S^P_A} S^P_A + U^{S_A}_{S^P_A}} + \frac{c^{2l}_{S_A} B^{S_A}_{\sigma^H} U^{S_A}_{S^P_A} \sigma^H + c^{2h}_{S_A} B^{S_A}_{S^P_A} B^{S_A}_{\sigma^H} S^P_A \sigma^H}{(B^{S_A}_{S^P_A} S^P_A + U^{S_A}_{S^P_A})(B^{S_A}_{\sigma^H} \sigma^H + U^{S_A}_{\sigma^H})} - 2\phi^{S_A}_{A^P} A^P S_A - 2\phi^{S_A}_{K^P} K^P S_A$$
$$+ 2\phi^{K}_{S^P_A} S^P_A K + 2\psi_{S^P_A} S^P_A + 2\phi^{P_h}_{S^P_A} P_h S^P_A - (r(1 - N_v/\kappa) + \lambda_{S_A}) S_A, \tag{5}$$

$$\frac{dS^P_A}{dt} = \phi^{S_A}_{K^P} K^P S_A - \phi^{K}_{S^P_A} S^P_A K + \phi^{S_A}_{A^P} A^P S_A - \phi^{P_h}_{S^P_A} P_h S^P_A - (r(1 - N_v/\kappa) + \psi_{S^P_A} + \lambda_{S^P_A}) S^P_A, \tag{6}$$

$$\frac{dK}{dt} = \frac{c_K H}{H + 1} - \alpha K + \phi^{S_A}_{K^P} K^P S_A - \phi^{K}_{S^P_A} S^P_A K + \psi_{K^P} K^P - (r(1 - N_v/\kappa) + \lambda_K) K, \tag{7}$$

$$\frac{dK^P}{dt} = \alpha K - \phi^{S_A}_{K^P} K^P S_A + \phi^{K}_{S^P_A} S^P_A K - (r(1 - N_v/\kappa) + \psi_{K^P} + \lambda_{K^P}) K^P, \tag{8}$$

$$\frac{dP_h}{dt} = c_{P_h} - \phi^{P_h}_{S^P_A} P_h S^P_A + \psi_{P^P_h} P^P_h - (r(1 - N_v/\kappa) + \lambda_{P_h}) P_h, \tag{9}$$

$$\frac{dP^P_h}{dt} = \phi^{P_h}_{S^P_A} P_h S^P_A - (r(1 - N_v/\kappa) + \psi_{P^P_h} + \lambda_{P^P_h}) P^P_h, \tag{10}$$

$$\frac{dA_b}{dt} = \frac{1}{4}\left(\frac{c^1_{A_b} U^{A_b}_{A_b}}{B^{A_b}_{A_b} A_b + U^{A_b}_{A_b}} + \frac{c^2_{A_b} U^{A_b}_{S^P_A}}{B^{A_b}_{S^P_A} S^P_A + U^{A_b}_{S^P_A}} \right) - (r(1 - N_v/\kappa) + \lambda_{A_b}) A_b, \tag{11}$$

$$\frac{d\sigma^H}{dt} = \frac{c_{\sigma^H} U^{\sigma^H}_{A_b}}{B^{\sigma^H}_{A_b} A_b + U^{\sigma^H}_{A_b}} - (r(1 - N_v/\kappa) + \lambda_{\sigma^H}) \sigma^H. \tag{12}$$

To reflect growth of the population, all intracellular variables are subject to dilution as modelled by the inclusion of the coefficient $r(1-N_v/\kappa)$. Assuming, for definiteness, that all proteins begin at the same concentration, we use the initial condition 10^4 nM for all variables listed above. Further biological data would inform a more accurate choice of initial conditions which, following our numerical investigations, appear to influence the timing of sporulation and solventogenesis: lower values delay the onset of both these processes.

In order to model AgrA influence over Spo0A∼P levels, the above formulation assumes the most direct interaction, i.e. that AgrA∼P phosphorylates Spo0A. There are, however, a number of other

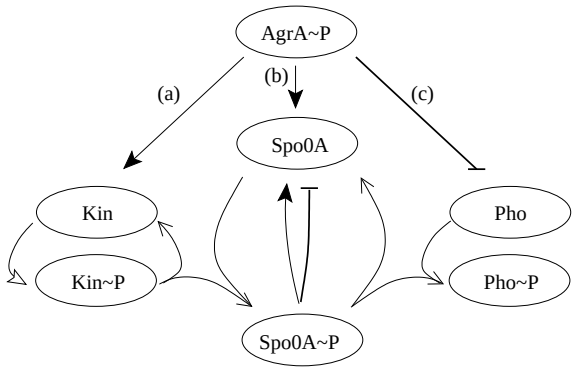

Figure 2: Schematic representations of the additional modes of interaction which we have considered in our investigations: (a) AgrA∼P increases transcription of the gene associated with the putative kinase; (b) AgrA∼P increases transcription of *spo0A*; (c) AgrA∼P inhibits transcription of the gene associated with the putative phosphatase. Arrow types correspond with Figure 1. Since the scenario depicted in Figure 1 (AgrA∼P phosphorylates Spo0A) yields the most interesting results, we focus the numerical simulations given here upon this model. However, each of the above scenarios is equally plausible *a priori* and we therefore include relevant simulations for all the corresponding models in Appendix A and detail any noteworthy behaviour arising from these in the main text.

ways by which the *agr* system could affect Spo0A∼P levels. Indeed, in *S. aureus*, AgrA∼P induces a response through altering the transcription of target virulence-related genes (for information on the targets of *agr* systems in other bacteria, see [30] for example) and it is plausible that this is also the method of interaction in *C. acetobutylicum*. Thus, the three additional scenarios which we consider are:

- AgrA∼P increases transcription of *spo0A*;
- AgrA∼P increases transcription of the gene associated with the putative kinase;
- AgrA∼P inhibits transcription of the gene associated with the putative phosphatase;

(these are illustrated in Figure 2) and we have extended our investigations to cover each of these possibilities. The extensive nature of these investigations precludes the inclusion of all relevant simulations. The model presented in this section produces the most interesting mathematical results and so we present these in full (we note that this is not because we assume this to be the correct interaction). For each of the remaining three models, we summarise the corresponding results in §3 (illustrating simulations only when unusual behaviour arises), and detail the relevant equations, alongside corresponding simulations, in Appendix A (thus, unless explicitly stated otherwise, the results below correspond to equations (5)–(12)).

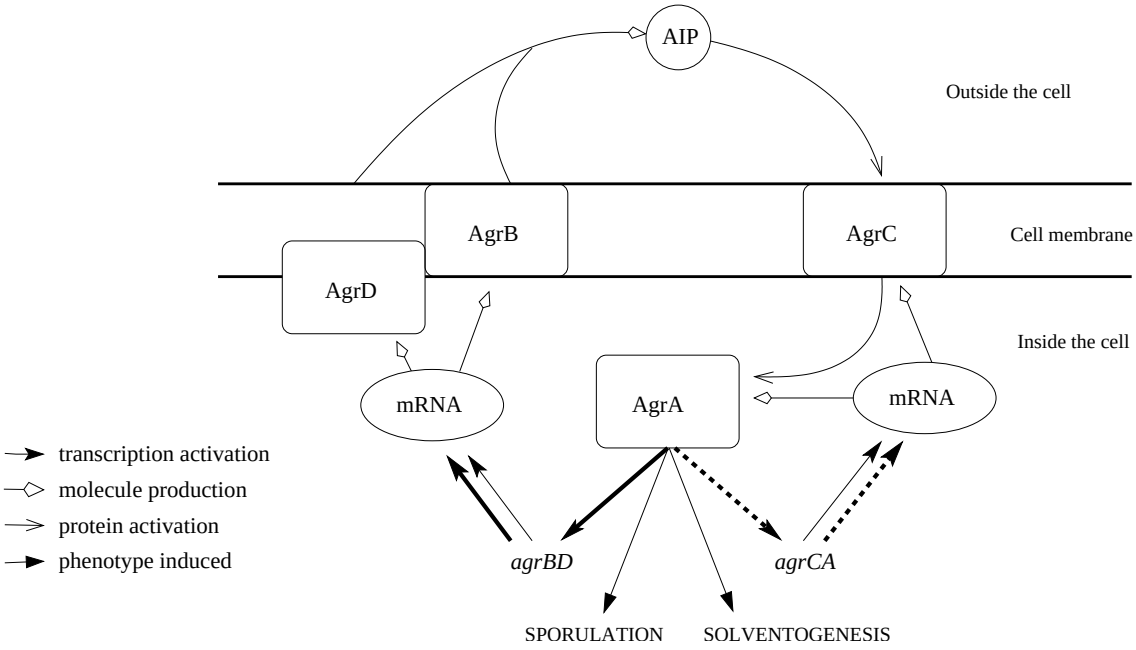

Figure 3: A schematic representation of the *agr* circuitry and its putative influence upon sporulation and solventogenesis in *C. acetobutylicum* (solid arrows). Quorum-sensing induced transcription is illustrated by the thick arrows (with the corresponding thin ones representing constitutive transcription). Unlike in *C. acetobutylicum*, in addition to constitutive transcription, in *S. aureus agrCA* is also transcribed at a higher rate as a quorum-sensing response; this is marked on the diagram with dashed arrows.

2.4. The agr operon

The *agr* system in *S. aureus* consists of four genes, namely *agrBDCA*, encoding the gene products AgrB, AgrD, AgrC and AgrA, see Figure 3. AgrB is a transmembrane protein which processes the AgrD propeptide to generate a quorum-sensing signal molecule which, in the case of the staphylococci, is a small modified peptide called an AIP (autoinducing peptide). The AIP is secreted into the external environment, where, upon accumulation, it is detected by a receptor protein (AgrC) present in the bacterial cell membrane. AIP binding to AgrC induces activation of AgrA, a DNA-binding protein. AgrA and AgrC are, respectively, the response regulator and sensor kinase of a two-component system. We assume the two-component system to take on a classical form, whereby AgrC autophosphorylates on reception of the AIP and subsequently transfers this phosphate to the response regulator AgrA. Phosphorylated (and thus activated) AgrA (AgrA$\sim$P) binds to the DNA binding site on the *agr* operon. In *S. aureus*, this leads to upregulation of all four *agr* genes. In *C. acetobutylicum*, on the other hand, although adjacent, *agrBD* and *agrCA* are predicted to form independent transcriptional units [31] and, accordingly, transcriptome data of [17] illustrate that only transcripts of *agrBD* are significantly increased at stationary phase. Thus

the evidence suggests that quorum sensing feedback into *agrCA* is absent in *C. acetobutylicum*.

In previous publications [16, 19] we have described and investigated a model of the *agr* operon with a view to developing novel techniques for combating staphylococcal pathogenesis. For this study we adapt the dimensional model described in Figure 4 of [16]. To bring the model in line with the sporulation initiation module, the proportion of *agr* up-regulated cells and the mRNA concentration (P and M from [16]) are taken to be quasi-steady. In addition the term representing mRNA transcribed from *agrCA* must be adapted from [16] to account for the difference in feedback between *S. aureus* and *C. acetobutylicum*. Thus we take

$$m_{BD} = c^l_{agr} + \frac{c^h_{agr} A^P}{A^P + U^{agr}_{A^P}/B^{agr}_{A^P}}, \quad m_{CA} = c^{CA}_{agr},$$

where m_{BD} is mRNA transcribed from *agrBD*, and m_{CA} that from *agrCA*. Following the analysis of [16], we replace D (the total amount of cytoplasmic AgrD in the population) by B (total amount of cytoplasmic AgrB) throughout, i.e. the numbers of these proteins in their cytoplasmic forms are assumed to be identical (notice that in [16] it was also possible to replace C by D, but absence of the feedback loop into *agrC* prevents that in this study). We remark that the parameters m, v, b, u of [16] are replaced by $c^l_{agr}, c^h_{agr}, B^{agr}_{A^P}, U^{agr}_{A^P}$ in this study, with the first two referring to transcription of *agrBD* only; c^{CA}_{agr} is introduced to represent transcription from *agrCA*.

The resulting equations are

$$\frac{dA}{dt} = c^{CA}_{agr} - \phi^A_{R^P} A R^P + \phi^{S_A}_{A^P} A^P S_A + \psi_{A^P} A^P - (r(1 - N_v/\kappa) + \lambda_A)A, \tag{13}$$

$$\frac{dA^P}{dt} = \phi^A_{R^P} A R^P - \phi^{S_A}_{A^P} A^P S_A - (r(1 - N_v/\kappa) + \psi_{A^P} + \lambda_{A^P})A^P, \tag{14}$$

$$\frac{dB}{dt} = c^l_{agr} + \frac{c^h_{agr} B^{agr}_{A^P} A^P}{B^{agr}_{A^P} A^P + U^{agr}_{A^P}} - (r(1 - N_v/\kappa) + \mu_{agr} + \lambda_B)B, \tag{15}$$

$$\frac{dC}{dt} = c^{CA}_{agr} - (r(1 - N_v/\kappa) + \mu_{agr} + \lambda_C)C, \tag{16}$$

$$\frac{dS}{dt} = \mu_{agr} B - k_{agr} T S - (r(1 - N_v/\kappa) + \lambda_S)S, \tag{17}$$

$$\frac{dT}{dt} = \mu_{agr} B - (r(1 - N_v/\kappa) + \lambda_T)T, \tag{18}$$

$$\frac{da}{dt} = k_{agr} T S - \beta_{R^P} R a + \gamma_{R^P} R^P - (\delta^a_H H + \delta^a_{S_v} S_v + \lambda_a)a, \tag{19}$$

$$\frac{dR}{dt} = \mu_{agr} C - \beta_{R^P} R a + \gamma_{R^P} R^P - (r(1 - N_v/\kappa) + \lambda_R)R, \tag{20}$$

$$\frac{dR^P}{dt} = \beta_{R^P} R a - (r(1 - N_v/\kappa) + \gamma_{R^P} + \lambda_{R^P})R^P. \tag{21}$$

As in §2.3, we take the initial conditions to be 10^4 nM for all of the variables listed above.

2.5. Parameter values

We assume that parameters concerning the sporulation-initiation network are transferable between *B. subtilis* and *C. acetobutylicum* and accordingly take these parameters directly from [9].

We do, however, as a result of our numerical investigations, choose an alternative default value for c_K, the rate of production of the kinase: in order for us to be able to view any effect of the *agr* system (since this is the aspect of the network on which this study is focused), this must be lower than our standard default value for low production of proteins (this being 0.4 nM sec^{-1} in [9]). We thus choose $c_K = 0.1$ nM sec^{-1} to be the default value in this study, but in §3 we illustrate the consequences of variations to this parameter (remember that c_K can represent the strength of additional sporulation- and solventogenesis-related signals).

Since our parameter choice in [9] covers protein production, degradation, phosphorylation, dephosphorylation, complex formation and separation, we extend this choice to cover the parameters governing the *agr* network. The only additional parameters required are c_{agr}^{CA}, μ_{agr} and k_{agr} which we take to be 4 nM sec^{-1}, 1 sec^{-1} and 0.4 $\text{nM}^{-1}\text{sec}^{-1}$, respectively. The first is chosen (following numerical investigations) to be sufficiently low for the *agr* genes not to be automatically up-regulated, but sufficiently high to be effective. The second is chosen for simplicity and the final value so that AIP production is comparable with protein production. Since these three parameters are not guided by the literature or experimental data, in Appendix B we investigate the effects of altering these parameters.

The remaining parameters concern the cell phenotype and are all estimated (except μ_e and μ_i) by fitting the models to experimental data from [14]. We note here that if we were to model an alternative interaction between AgrA∼P and Spo0A or *spo0A* (e.g. through transcription instead of phosphorylation), certain of these parameters differ and we list these in Appendix A. We anticipate that μ_e and μ_i (the rates of acid/solvent externalisation and internalisation) will be comparable to each other and set them to 1 sec^{-1}. Examination of equations (3) and (4) shows that if $\mu_e = \mu_i$, their actual value is irrelevant since they only appear in the form $\mu_e/(\mu_e + \mu_i)$ or μ_i/μ_e.

The default parameter set is given in Table 3.

3. Numerical solutions

3.1. The impact of the clostridial agr system upon sporulation and solventogenesis

In Figure 4 we illustrate a numerical solution to the full system using the default parameter set and initial conditions. The dynamics of the model are able to describe well our experimental observations: vegetative cell numbers increase before high acid levels (and eventually high solvent levels) cause cell death; some cells survive in the form of spores, while acids are converted into solvents. There are two main failings of the model and these are discussed in the caption. We note that the three additional models can also reproduce this behaviour with slightly different values of ρ and ξ (see Figures A.12(a)–A.14(a) in Appendix A).

Parameters associated with	Parameter	Default Value	Units
Production	c_H	8×10^{-6}	nM cells^{-1} ml sec^{-1}
	c_K	0.1	nM sec^{-1}
	$c^l_{agr}, c^1_{S_A}, c^{2l}_{S_A}, c_{P_h}, c^1_{A_b}, c^2_{A_b}, c_{\sigma^H}$	0.4	nM sec^{-1}
	k_{agr}	0.4	nM^{-1} sec^{-1}
	c^{CA}_{agr}	4	nM sec^{-1}
	$c^h_{agr}, c^{2h}_{S_A}$	40	nM sec^{-1}
DNA binding and unbinding	U^Y_X/B^Y_X for all relevant X, Y	20	nM
Complex separation	γ_{R^P}	0.1	sec^{-1}
Complex formation	β_{R^P}	0.083	nM^{-1} sec^{-1}
Degradation	$\lambda_{S^P_A}$	10^{-5}	sec^{-1}
	λ_{σ^H}	0.0004	sec^{-1}
	$\lambda_A, \lambda_{A^P}, \lambda_B, \lambda_S, \lambda_T, \lambda_R, \lambda_{R^P},$	0.002	sec^{-1}
	$\lambda_K, \lambda_{K^P}, \lambda_{S_A}, \lambda_{A_b}$	0.002	sec^{-1}
	λ_a	0.02	sec^{-1}
Autophosphorylation	α	0.1	sec^{-1}
Phosphotransfer	$\phi^{S_A}_{K^P}, \phi^K_{S^P_A}, \phi^{S_A}_{A^P}, \phi^{P_h}_{S^P_A}, \phi^A_{R^P}$	10^{-6}	nM^{-1} sec^{-1}
Dephosphorylation	$\psi_{A^P}, \psi_{K^P}, \psi_{S^P_A}\psi_{P^P_h}$	0.0004	sec^{-1}
Transport	μ_e, μ_i	1	sec^{-1}
Movement to cell membrane	μ_{agr}	1	sec^{-1}
Growth	r	1.67516×10^{-4}	sec^{-1}
	κ	7.29057×10^{8}	cells ml^{-1}
Cell death	δ_H, δ^a_H	1.03×10^{-12}	nM^{-1} sec^{-1}
	$\delta_{S_v}, \delta^a_{S_v}$	9×10^{-13}	nM^{-1} sec^{-1}
Spore formation	ξ	2×10^{-10}	nM^{-1} sec^{-1}
Acid conversion	ρ	2×10^{-8}	nM^{-1} sec^{-1}

Table 3: The default parameter set.

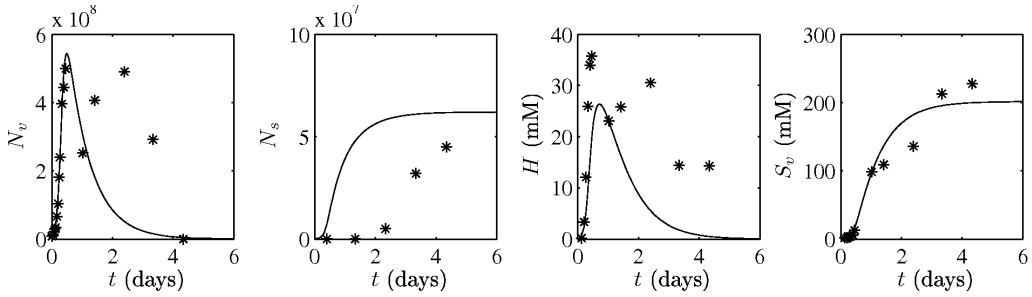

Figure 4: Numerical solution (solid line) to the model given by equations (1)–(21) using the default parameter set displayed in Table 3; we will refer to this henceforth as the wild-type solution. In the interests of brevity, we display only those variables related directly with cell phenotype: vegetative cells, spores, acid concentration and solvent concentration. The asterisks illustrate data taken from [14] (converted to represent vegetative and spore cells, as discussed in §2.2). Early cell growth, acid production and solventogenesis are represented well by the model, which simulates spore formation too fast (this is likely to explain the lack of fit of vegetative cells in later growth and may be due either to our assumption that sporulation occurs at a rate that is linearly proportional to Spo0A∼P levels, or to the absence from the model of the pathways involved in sporulation initiation that are downstream of Spo0A). In addition, the model does not achieve a non-zero steady state for acid levels; this can be fixed by imposing a constraint upon acid conversion: above a threshold solvent level, this process is aborted (results not shown). Further experimental data (namely at a subcellular level) are required to inform an improved fit but the phenotypic trends are captured sufficiently well for hypotheses to be drawn from the model.

In Figures 5(a) and (b), we demonstrate the numerical solutions if we knock out, respectively, the kinase or the *agr* system from the model. The former has little impact upon the solution, while the second knock-out (that of the quorum-sensing system) drastically lowers the spore count while slowing down the solventogenic response. Thus, under the default parameter set, the *agr* system is driving both survival strategies. A minor alteration to the parameter set, however, can enable the kinase to be effective (see the dotted line of Figure 5(b)), meaning that both phenotypes can be controlled by either the *agr* system or by the kinase.

In the three alternative networks, removing the kinase from the system removes the only source of phosphate for Spo0A; hence such a comparison is not practical as no Spo0A∼P can be formed and neither phenotype can be induced. Removal of the *agr* system in the cases in which AgrA∼P affects either production of the kinase or of the phosphatase, leads to results qualitatively equivalent to those above – see Figures A.13(b)–A.14(b) in Appendix A. If AgrA∼P increases transcription of *spo0A*, however, the consequences of an *agr* knock-out differ: a wild-type-like response remains, see Figure 6. If $c_K = 0.1$, the kinase dominates over the *agr* response; lowering c_K does enable *agr* to be effective, however, see the dotted line of Figure 6. This suggests that in this case the influence of AgrA∼P via transcription of *spo0A* is the weakest of the four scenarios (in further evidence of this, the rates of spore formation and acid conversion must be faster than those of the

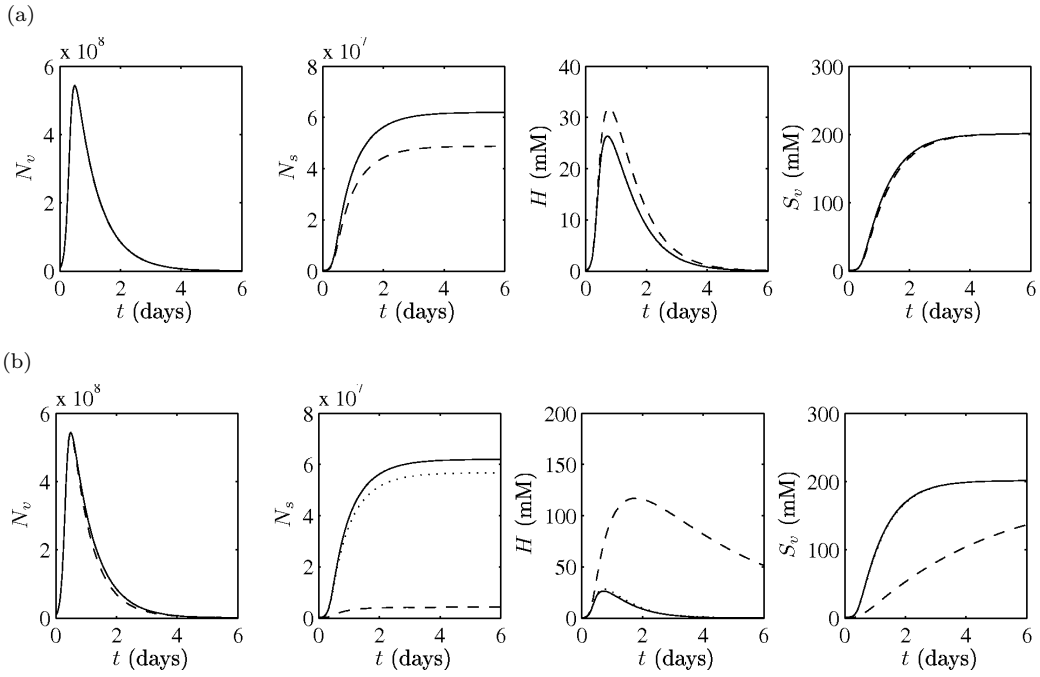

Figure 5: Solid line: numerical solution to the model given by (1)–(21), using the default parameter set and initial conditions, i.e. the wild-type solution. (a) Dashed line: numerical solution when $c_K = 0$ and $K(0) = K^P(0) = 0$, i.e. a simulation of a kinase knock-out (indistinguishable from the solid line for N_v). It is evident that, under this parameter choice, both phenotypes (sporulation and solventogenesis) arise in spite of the absence of the kinase, implying that, in this scenario, it is not the kinase which is responsible for triggering either response. (b) Dashed line: numerical solution when $c^l_{agr} = c^h_{agr} = c^{CA}_{agr} = 0$ and $A(0) = A^P(0) = B(0) = C(0) = S(0) = T(0) = R(0) = R^P(0) = a(0) = 0$, i.e. a representation of an *agr* mutant. Removal of the *agr* proteins prevents sporulation and greatly slows down solventogenesis under our chosen parameter set. Dotted line: as for the dashed line with the exception that c_K is raised from 0.1 nM sec^{-1} to 0.5 here (the dotted line is indistinguishable from the solid line for N_v, H and S_v). This change enables the kinase to be effective and induces both phenotypes without any input from the *agr* system.

other three models for this model to reproduce results qualitatively similar to our experimental data).

Interestingly, induction of the two phenotypes can be split: they need not occur simultaneously. Reducing ρ, the rate of solvent formation from acids, results in the *agr* system causing sporulation, but not solventogenesis (at least on the timescale with which we are concerned); increasing the rate of kinase production can restore solventogenesis – see Figure 7 (here we return to the network where AgrA∼P phosphorylates Spo0A). Similarly, reducing ξ, the rate of spore formation, prevents the *agr* system from triggering sporulation while solventogenesis does occur (see Figure 8, solid line), but, crucially, ξ must be sufficiently small that sporulation is not restored by increasing the rate at which the kinase is produced (Figure 8, dashed line). Thus, the scenario whereby

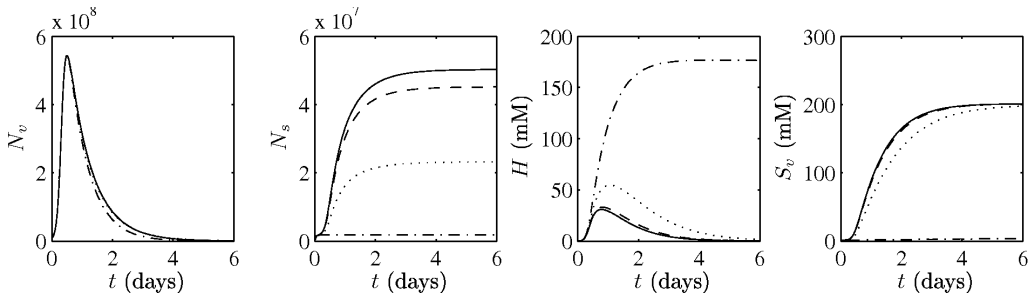

Figure 6: Numerical solution when AgrA∼P activates transcription of *spo0A*. Solid line: wild-type solution; dashed line: simulation of an *agr* mutant; dot-dash line: an *agr* mutant with c_K lowered to 0.08 nM sec^{-1}; dotted line: wild-type solution with $c_K = 0.08$ nM sec^{-1}. In this scenario (and under the default parameter set), the kinase is more influential over the phenotypes than is the *agr* system, in contrast to the case in which AgrA∼P phosphorylates Spo0A.

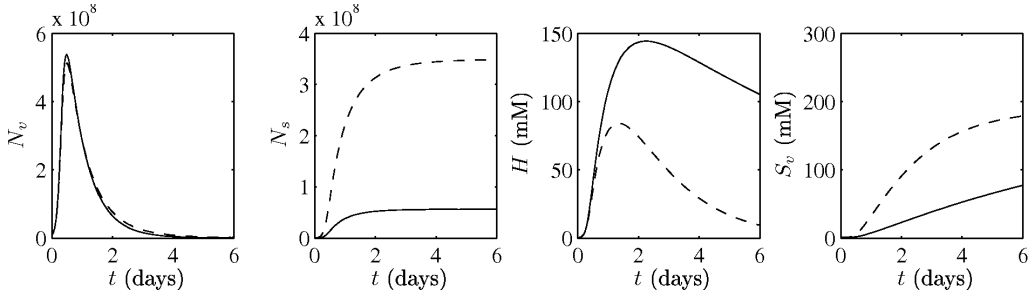

Figure 7: Solid line: numerical solution for the wild-type model (when AgrA∼P is capable of phosphorylating Spo0A) with all parameters except ρ, which is decreased to 5×10^{-10} nM^{-1} sec^{-1}, taken from the default parameter set. Dashed line: as above with c_K increased to 4 nM sec^{-1}. The solid line illustrates a parameter choice whereby the *agr* system can initiate sporulation but not solventogenesis and, from the dashed line, we see that increased transcription of the kinase gene (which could occur as a result of some additional input signal) could reinstate solventogenesis.

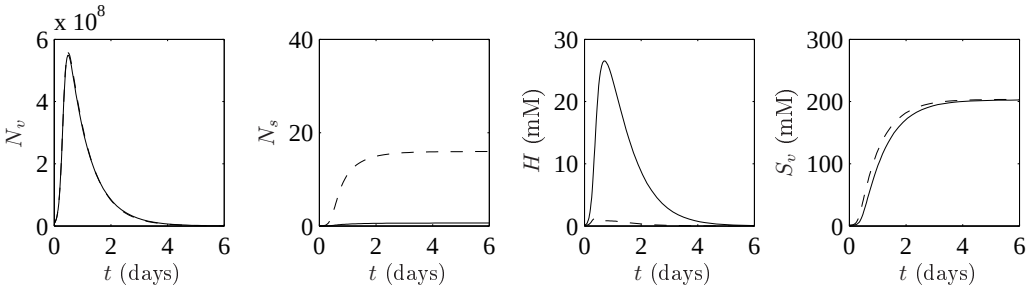

Figure 8: Solid line: numerical solution to the wild-type model with all parameters except ξ (which we decrease to 2×10^{-18} nM^{-1} sec^{-1}) taken from the default parameter set. Dashed line: as above with c_K increased to 10^6 nM sec^{-1}. In a similar manner to Figure 7, we see the phenotype responses being separated: here solventogenesis arises without the formation of any substantial number of spores. The key difference from Figure 7 is that ξ must be so small for sporulation not to arise that additional kinase transcription does not enforce sporulation.

the *agr* system can induce solventogenesis but not sporulation is somewhat unlikely; moreover if *agr* affects only one of the phenotypes, of the two possibilities it seems more likely that *agr* only induces sporulation. These conclusions apply to all of the interactions between AgrA∼P and the sporulation-initiation network noted above, i.e. also to those models detailed in Appendix A (see Figures A.12(c,d)–A.14(c,d)) and are consistent with the experimental findings of [14].

The fact that the kinase and *agr* systems can interact to generate qualitatively distinct responses depending upon the transcription rates of the corresponding genes suggests that the overall network is set up well to perceive multiple signals and react accordingly (something which is crucial for the appropriate onset of survival mechanisms); we shall see in §3.2 that modifications to the *agr* circuit may obstruct this. Furthermore, the network as it stands reacts to additional signals even when the *agr* system is switched on, see Figure 9, with the response levels of both solventogenesis and sporulation increasing with kinase transcription rate (this also applies to the additional three networks, Figures A.12(e)-A.14(e)). In fact, increasing c_K in each of the models where AgrA∼P acts via transcription, enhances spore count to such an extent that vegetative cell number is significantly lowered. Hence the number of spores and the speed at which solventogenesis occurs both correlate with the intensity of the need for either survival mechanism: the more signals there are that indicate an unfavourable environment for vegetative cells, the more spores that will be formed to maximise the chances of creating a surviving population. The networks appear, therefore, to be well suited to dealing with multiple signals.

3.2. The S. aureus agr system

Many previously studied *agr* systems conform to the standard type first discovered in *S. aureus* whereby transcription of each element in the *agr* system is up-regulated as a result of increased

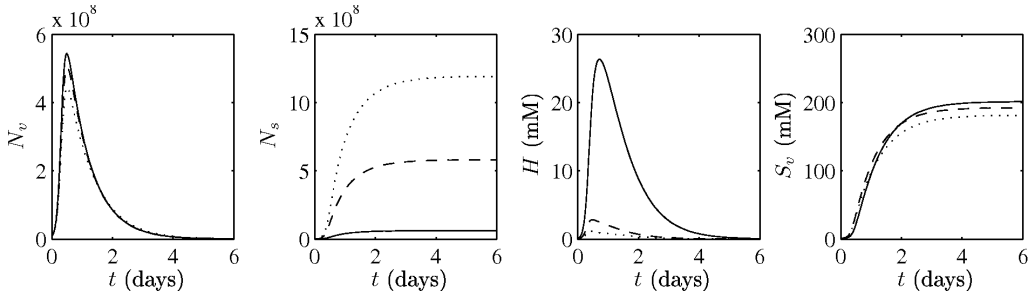

Figure 9: Solid line: wild-type solution; dashed line: $c_K = 10$ nM sec^{-1}; dotted line: $c_K = 1000$. Additional signals feeding into the kinase can increase the rate at which solventogenesis occurs and the number of spores that are formed.

population density. *C. acetobutylicum*, however, does not match this type: only the elements connected with signal production are affected by fluctuations in population density. Existing models of the *agr* system point to the upregulation of the two-component system elements (i.e. those concerned with signal detection as opposed to signal production) as being the crucial requirement for upregulation of the system as a whole [16]. Thus it is curious that *C. acetobutylicum* has evolved a quorum-sensing system which could be deemed to be less efficient. In order to examine this phenomenon, we compare the results of §3.1 with those that would arise were an *agr* system with all elements (i.e. *agrBD* **and** *agrCA*) subject to upregulation in *C. acetobutylicum*. We use the default parameter set found in Table 3 (i.e. identical parameters to those used for the previous simulations) unless stated otherwise but the same qualitative conclusions concerning splitting the phenotypes and incorporating additional signals (see below) hold if ρ and ξ are chosen so that the *S. aureus agr* system induces a more biologically realistic response, i.e. to be quantitatively in line with the wild-type solution of §3.1.

In Figure 10, we see that the *S. aureus agr* system would result in a far greater number of spores and a much earlier onset of solventogenesis. As for the original model, Figures 11(a) and (b) demonstrate that minor alterations to the parameter set enable either sporulation or solventogenesis to be induced without the other. Crucially, however, neither phenotype can be restored through increased production of the kinase: the strength of the *S. aureus agr* circuit is so great that, to prevent it from triggering a specific phenotype, the corresponding parameter (ρ for solventogenesis and ξ for sporulation) must be reduced so significantly that a much increased level of signal is not able to induce it (the effect of signals is saturated through the network so it is not simply a case of increasing the signal to induce a greater response). Thus the *S. aureus agr* system is in effect too powerful to manifest appropriate interactions with the other signals. Additionally, we see from Figure 11(c) that the *S. aureus agr* system gives the maximal response when *agr*

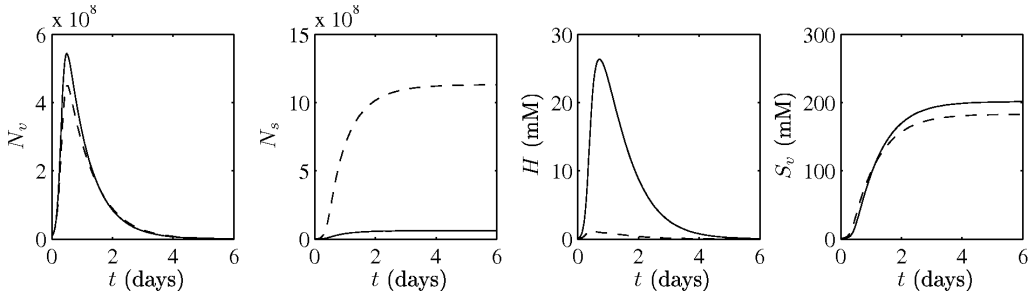

Figure 10: Solid line: wild-type solution for (1)–(21), i.e. using the *agr* system of *C. acetobutylicum*. Dashed line: the numerical solution when (13) and (16) are modified to represent the *agr* circuitry as found in *S. aureus*. The alterations to the *agr* circuitry result in a far greater number of spores and solventogenesis occurring at a much faster rate.

is effective: no significant augmentation in spore number or speed of solventogenesis can occur through the presence of more signals. By contrast, the *agr* circuit used by *C. acetobutylicum*, has the capacity to tune spore numbers to reflect the hostility of the environment to vegetative cells; this provides a possible explanation as to why *C. acetobutylicum* has evolved an *agr* system of the modified form to deal with surviving conditions which are unfavourable to vegetative growth. These results comparing the two types of *agr* system are applicable, however, only to the case in which AgrA∼P leads to the phosphorylation of Spo0A. The other three networks (whereby the interaction is through alteration in transcription rates and not phosphorylation) behave quite differently: in each of the three cases, the influence of the modified *agr* system (i.e. that of *C. acetobutylicum*) on sporulation and solventogenesis appears to be almost identical to that of the *S. aureus agr* system – neither the spore count nor the rate at which solventogenesis occurs can be increased through the addition of positive feedback into the transcription of *agrA* and *agrC* (occurring in accordance with population density). Thus it would seem that the effect of *agr* upon the overall sporulation-initiation network is somewhat diluted if the method of interaction is via transcription rather than phosphorylation, presumably because the transcription rate of a particular gene is limited, whereas phosphorylation can occur freely as long as the two relevant substrates are in plentiful supply.

4. Summary

Building upon previous models [9, 16], we have developed a model representing *C. acetobutylicum* in batch culture. Under these conditions the cells initially use acid fermentation as an energy-yielding process. However, a sufficiently acidic environment will cause the cells to die. Thus, after a period of time, the cells switch to solventogenesis which involves the uptake of the

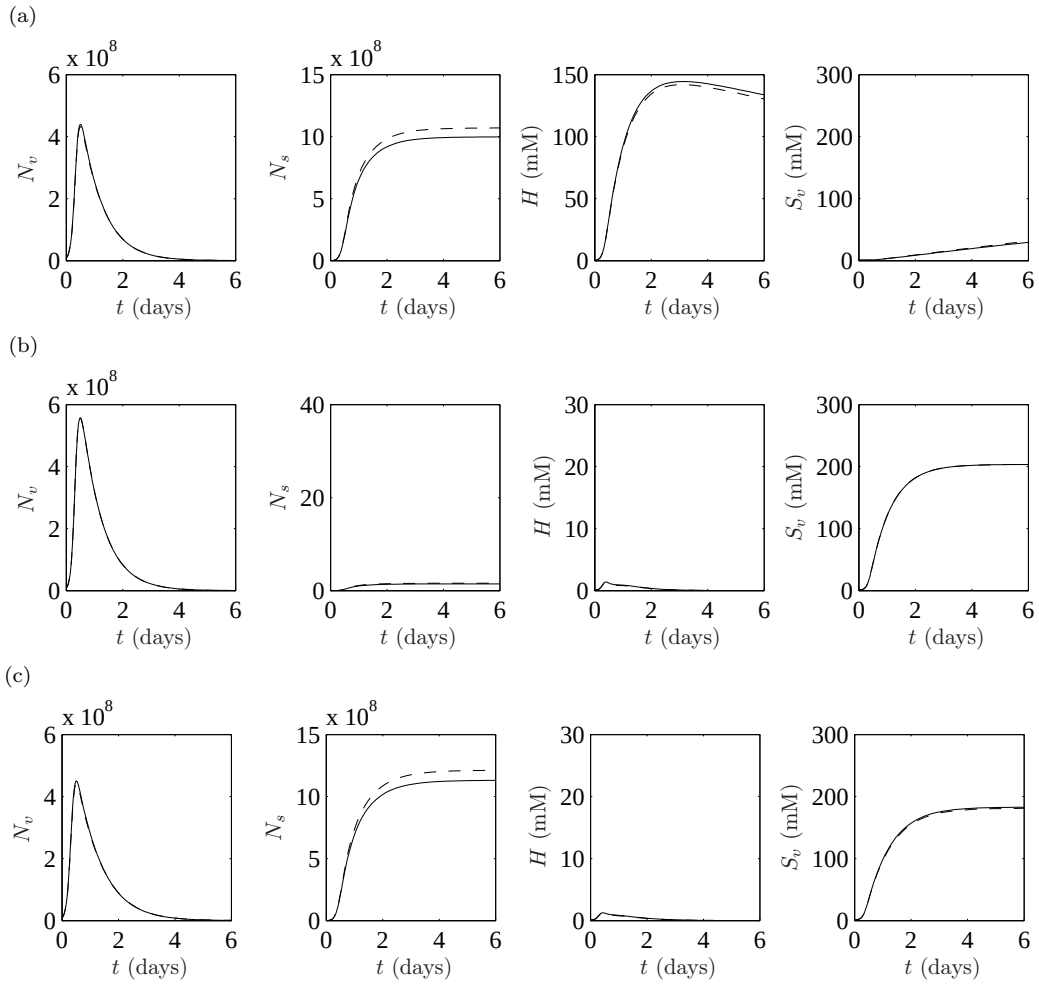

Figure 11: (a) Solid line: numerical solution for the *S. aureus agr* circuitry model (as in the dashed line of Figure 10) with all parameters except ρ, which we decrease to 10^{-11} nM^{-1} sec^{-1}, taken from the default parameter set. Dashed line: as above with c_K increased to 10^6 nM sec^{-1}. The solid line illustrates a parameter choice whereby the *agr* system can initiate sporulation but not solventogenesis and, from the dashed line, we see that increased transcription of the kinase gene does not reinstate solventogenesis. (b) Solid line: numerical solution for the *S. aureus agr* circuitry model (as in the dashed line of Figure 10 with all parameters except ξ, which we decrease to 2×10^{-19} nM^{-1} sec^{-1}, taken from the default parameter set). Dashed line: as above with c_K increased to 10^6 nM sec^{-1} (though these results are indistinguishable from the solid line). The phenotype responses are separated: here solventogenesis arises without the formation of any substantial number of spores. As with the wild-type solution in Figure 7, ξ must be so small for sporulation not to arise that additional kinase transcription does not enforce sporulation. (c) Solid line: numerical solution for the *S. aureus agr* circuitry model (as in the dashed line of Figure 10 with the default parameter set). Dashed line: c_K is raised to 10^6 nM sec^{-1}. It is evident that, if the *S. aureus agr* circuitry is switched on, any additional signal input will have negligible effect upon the phenotypes.

existing acids. Solventogenesis thus serves two purposes: it eliminates the acids from the environment allowing the cells to survive for longer, while also producing energy (though less efficiently than through acid production). The combination of these two processes effectively buys the cells time to form spores which are resistant to extreme pH, i.e. solventogenesis is a temporary survival mechanism (since the presence of solvents will also eventually result in cell death) facilitating the longer term (and more effective) survival mechanism that is sporulation.

We have described and simulated a model which is consistent with the hypothesis that the *agr* quorum-sensing system could trigger the solventogenesis and sporulation responses in clostridial bacteria. In addition, we have demonstrated the plausibility of this system triggering either response in isolation, though it seems somewhat unlikely that the *agr* system does not induce sporulation given that the required rate of spore formation for *agr* not to induce sporulation is so slow that sporulation cannot even arise in response to additional signals. It is, however, quite plausible that the *agr* system affects sporulation but not solventogenesis, as is the case with *C. acetobutylicum* in [14].

Sporulation could arise in response to a number of signals. For instance, it is known that sporulation is affected by nutrient limitation, DNA damage and population density, amongst other factors, in *B. subtilis* (see [10] for example) and it is likely that a variety of environmental or cellular conditions also be involved in the 'decision-making' behind spore formation in *C. acetobutylicum*. Our results indicate that the sporulation-initiation network of *C. acetobutylicum* is well-suited to incorporating a variety of signals, with the number of cells assigned to the fate of sporulation increasing with the level of sporulation-inducing signal introduced to the system (this is represented by increases in the rate of production of the putative kinase, but could equally correspond to the production of one or more supplementary kinases). Additionally, the inclusion of a phosphorelay between the kinase or AgrA and Spo0A would increase the number of possible entry points for extra signals.

It is highly plausible that quorum sensing would be involved in the onset of solventogenesis and sporulation given that the denser the population the more toxic the environment would become through acid production; triggering either of these two processes initiates a survival mechanism (solventogenesis in the short term and sporulation in the long term) enabling the cells to survive the toxic environment for longer. Detailed experimental results (phenotypic and subcellular) demonstrating the effect of the *agr* system on either the solventogenesis or sporulation phenotypes in batch culture can be combined with modelling work (based upon that presented here) to help determine the mechanism by which AgrA interacts with the sporulation initiation network in a particular species. In addition, a full structural analysis of the model should yield simpler sub-models, generating further insight into the full network.

We have also examined the differences in behaviour between the *agr* circuitry of *C. acetobutylicum* and that of *S. aureus*. Our findings indicate that if AgrA∼P is capable of transferring its phosphate directly (or possibly via a phosphorelay) to Spo0A, then the modified circuitry of *C. acetobutylicum* allows the number of spores formed and the speed at which solventogenesis occurs to reflect the urgency for either of these processes. Sporulation, in particular, requires a great deal of energy and takes a considerable length of time, representing an extreme survival strategy. It is beneficial, therefore, for a cell to undergo sporulation only when strictly necessary and it is not required that every cell in a population follow this pathway: only enough spores to initiate a healthy vegetative population (once conditions have returned to being favourable) are needed. Moreover, it might be beneficial for a number of cells to remain in a vegetative state in case conditions unexpectedly become more favourable for cell growth. The *C. acetobutylicum agr* circuitry (induced by high population density) enforces sporulation in only a relatively small proportion of cells in the overall population; the number created as a result of the *S. aureus agr* system would be far greater, resulting in wasteful expense of energy by the population as a whole.

If AgrA∼P were to affect sporulation or solventogenesis via transcription, on the other hand, there appears to be little difference between the two *agr* systems: in our simulations, the *S. aureus* circuitry does not give a higher number of spores than the *C. acetobutylicum* circuitry, most likely because the effect of AgrA∼P becomes saturated in the transcription process. Thus if *agr* is found to affect sporulation or solventogenesis via alteration to the transcription of a target gene, it may be that the *C. acetobutylicum* circuitry has evolved simply because it requires less energy to function.

As it stands, therefore, our modelling work is capable of providing insight into the mechanisms and networks involved in sporulation initiation and solventogenesis in *C. acetobutylicum*. If the bacterium is to be manipulated to maximise butanol production for the manufacture of biofuels it will be necessary to understand these networks as fully as possible. Furthermore, results concerning the mechanisms of the *agr* system will be applicable to many more bacteria given the prevalence of such quorum-sensing systems in the bacterial domain of life, with the study of four distinct models being particularly important given the wide variation in regulators downstream of each *agr* system [30]. Many *agr* systems are associated with pathogenesis in highly virulent bacteria (for example, *S. aureus* or *C. difficile*), making our findings of broader importance. Currently, work is under way to identify additional key components of the sporulation-initiation network, it being likely that additional proteins are involved (such as a pH-related signal transduction mechanism) and the model is readily adaptable to incorporate these extra aspects as and when they are discovered.

Acknowledgements

The authors gratefully acknowledge support from BBSRC for this work, which was undertaken as

part of the COSMIC and COSMIC2 projects (Systems Biology of *C. acetobutylicum* - a possible answer to dwindling crude oil reserves) forming part of the SysMO and SysMO2 (Systems Biology of Microorganisms) initiatives. JRK also thanks the Royal Society and Wolfson Foundation for funding and SJ the MRC for a Biomedical Informatics Fellowship..

Appendix A. Additional putative interactions between AgrA and the sporulation-initiation network

In addition to the model presented in the main text of the paper, we have also investigated several other possibilities for the mode of contact between AgrA∼P (the activator of the *agr* system) and the sporulation-initiation network. In the main text, we have assumed that AgrA∼P can phosphorylate Spo0A (the response regulator of the network) since this is the simplest and most direct link to the induction of the sporulation and solventogenesis phenotypes and yields the most interesting results mathematically. The three most logical alternatives to this scenario are that AgrA∼P increases transcription of *spo0A* or the gene associated with the putative kinase, or, alternatively, decreases transcription of the putative phosphatase; indeed, in *S. aureus*, AgrA∼P is capable of binding to specific DNA to alter transcription of its target genes. Each of these scenarios could result in increased concentration of Spo0A∼P, meaning that AgrA∼P would have a positive effect upon the response regulator which triggers sporulation and solventogenesis; thus each are consistent with our experimental observations.

Our investigations, with minor alterations to the default parameter set employed in the main text (namely to ρ and ξ, see Table A.4), produce qualitatively equivalent results to those derived in §3 of the paper, unless explicitly stated otherwise. In the following sections, we present the models and a selection of numerical solutions (Figures A.12–A.14).

Phosphorylated AgrA increases transcription of spo0A

In the case where we consider that AgrA∼P increases transcription of the *spo0A* gene, the only equations which differ from (1)–(21) are (5),(6),(13),(14). These become

$$\begin{aligned}\frac{dS_A}{dt} &= \frac{c^1_{S_A}U^{S_A}_{S^P_A}}{B^{S_A}_{S^P_A}S^P_A + U^{S_A}_{S^P_A}} + \Big[c^{2l}_{S_A}B^{S_A}_{\sigma^H}U^{S_A}_{S^P_A}U^{S_A}_{A^P}\sigma^H \\ &\quad + c^{2h}_{S_A}(B^{S_A}_{\sigma^H}B^{S_A}_{S^P_A}U^{S_A}_{A_P}\sigma^H S^P_A + B^{S_A}_{\sigma^H}B^{S_A}_{A^P}U^{S_A}_{S^P_A}\sigma^H A_P + B^{S_A}_{\sigma^H}B^{S_A}_{S^P_A}B^{S_A}_{A_P}\sigma^H S^P_A A^P)\Big] \Big/ \\ &\quad \Big[(B^{S_A}_{S^P_A}S^P_A + U^{S_A}_{S^P_A})(B^{S_A}_{A^P}A^P + U^{S_A}_{A^P})(B^{S_A}_{\sigma^H}\sigma^H + U^{S_A}_{\sigma^H})\Big] \\ &\quad - 2\phi^{S_A}_{K^P}K^P S_A + 2\phi^K_{S^P_A}S^P_A K + 2\phi^{P_h}_{S^P_A}P_h S^P_A + 2\psi_{S^P_A}S^P_A - (r(1-N_v/\kappa)+\lambda_{S_A})S_A, \quad \text{(A.1)}\end{aligned}$$

$$\frac{dS^P_A}{dt} = \phi^{S_A}_{K^P}K^P S_A - \phi^K_{S^P_A}S^P_A K - \phi^{P_h}_{S^P_A}P_h S^P_A - (r(1-N_v/\kappa)+\psi_{S^P_A}+\lambda_{S^P_A})S^P_A, \quad \text{(A.2)}$$

$$\frac{dA}{dt} = c^{CA}_{agr} - \phi^A_{R^P}AR^P + \psi_{A^P}A^P - (r(1-N_v/\kappa)+\lambda_A)A, \quad \text{(A.3)}$$

$$\frac{dA^P}{dt} = \phi^A_{R^P}AR^P - (r(1-N_v/\kappa)+\psi_{A^P}+\lambda_{A^P})A^P. \quad \text{(A.4)}$$

Notice that the rather complicated term representing transcription of *spo0A* in (A.1) arises from the competitive binding of Spo0A∼P, σ^H and AgrA∼P at the DNA binding site of *spo0A* (see [9] for more explanation of this modelling technique). Numerical solutions for this model are displayed in Figure A.12.

Phosphorylated AgrA increases transcription of the putative kinase

If we assume that AgrA∼P can bind to the DNA binding site of the putative kinase, increasing its transcription and raising the number of kinase proteins within each cell, the equations which differ from the model presented in the main paper are (5), (6), (7), (13) and (14). The equations representing Spo0A∼P, AgrA and AgrA∼P are respectively given by (A.2), (A.3) and (A.4) above; (5) and (7) are replaced by

$$\begin{aligned}\frac{dS_A}{dt} &= \frac{c^1_{S_A}U^{S_A}_{S^P_A}}{B^{S_A}_{S^P_A}S^P_A + U^{S_A}_{S^P_A}} + \frac{c^{2l}_{S_A}B^{S_A}_{\sigma^H}U^{S_A}_{S^P_A}\sigma^H + c^{2h}_{S_A}B^{S_A}_{S^P_A}B^{S_A}_{\sigma^H}S^P_A\sigma^H}{(B^{S_A}_{S^P_A}S^P_A + U^{S_A}_{S^P_A})(B^{S_A}_{\sigma^H}\sigma^H + U^{S_A}_{\sigma^H})} \\ &\quad - 2\phi^{S_A}_{K^P}K^P S_A + 2\phi^K_{S^P_A}S^P_A K + 2\psi_{S^P_A}S^P_A + 2\phi^{P_h}_{S^P_A}P_h S^P_A - (r(1-N_v/\kappa)+\lambda_{S_A})S_A, \quad \text{(A.5)}\end{aligned}$$

$$\begin{aligned}\frac{dK}{dt} &= c_K\left(\frac{B^K_{A^P}A^P}{B^K_{A^P}A^P + U^K_{A^P}} + \frac{H}{H+1}\right) - \alpha K + \phi^{S_A}_{K^P}K^P S_A - \phi^K_{S^P_A}S^P_A K + \psi_{K^P}K^P \\ &\quad - (r(1-N_v/\kappa)+\lambda_K)K. \quad \text{(A.6)}\end{aligned}$$

Numerical solutions for this model are displayed in Figure A.13.

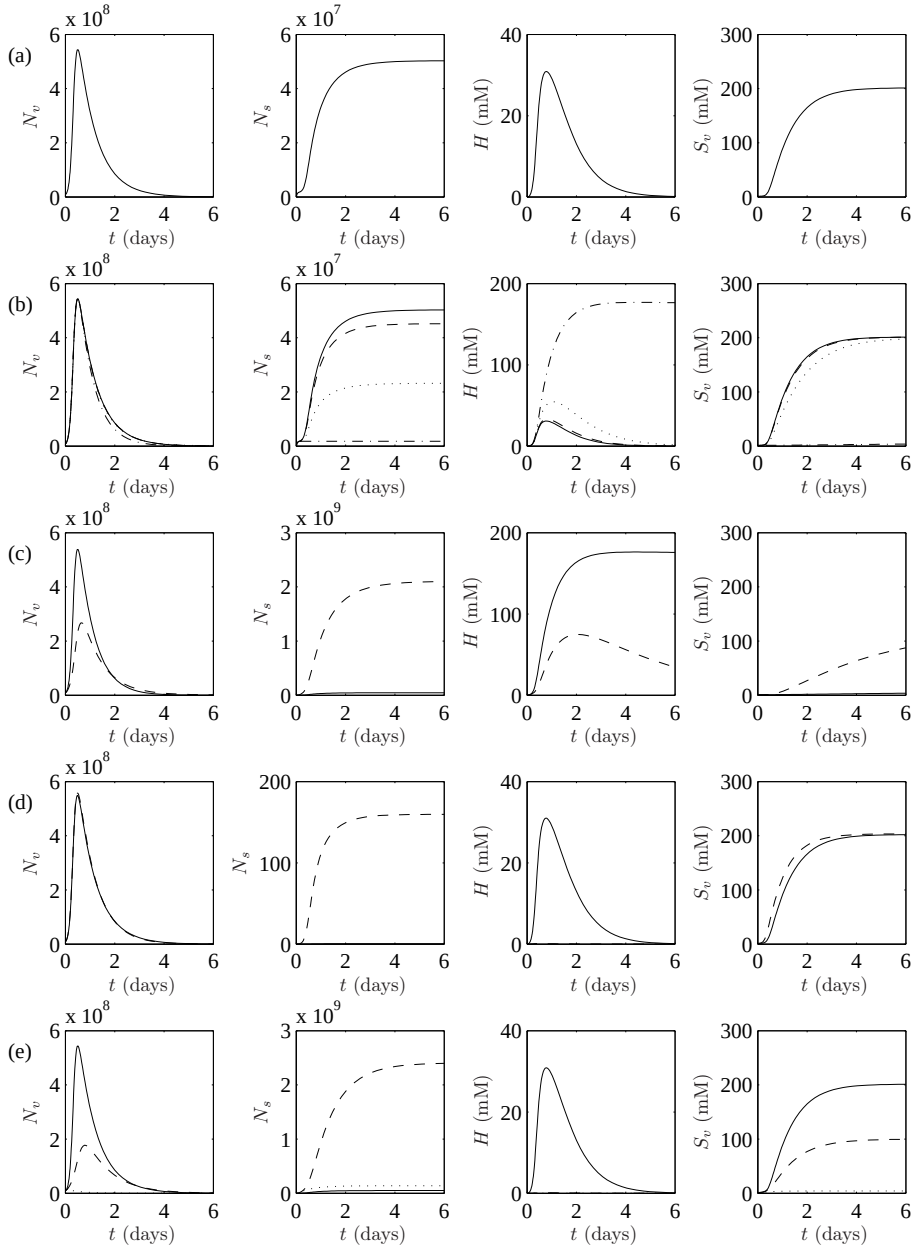

Figure A.12: Numerical solutions for the model whereby phosphorylated AgrA activates transcription of *spo0A*. (a) Wild-type solution ($\rho = 2 \times 10^{-7}, \xi = 2 \times 10^{-9}$). (b) Solid line: wild-type solution; dashed line: *agr* mutant; dot-dash line: *agr* mutant with $c_K = 0.08$ nM sec^{-1}; dotted line: wild-type solution with $c_K = 0.08$ nM sec^{-1}. (c) Default parameters except $\rho = 2 \times 10^{-10}$. Solid line: $c_K = 0.1$ (default); dashed line: $c_K = 5$. (d) Default parameters except $\xi = 2 \times 10^{-17}$. Solid line: $c_K = 0.1$ (default); dashed line: $c_K = 10^6$. (e) Wild-type solution. Solid line: $c_K = 0.1$ (default); dashed line: $c_K = 10$; dotted line: $c_K = 1000$ (note that increasing c_K to this degree causes spore formation so quickly that vegetative cell count is drastically reduced, resulting in fewer spores than for $c_K = 10$).

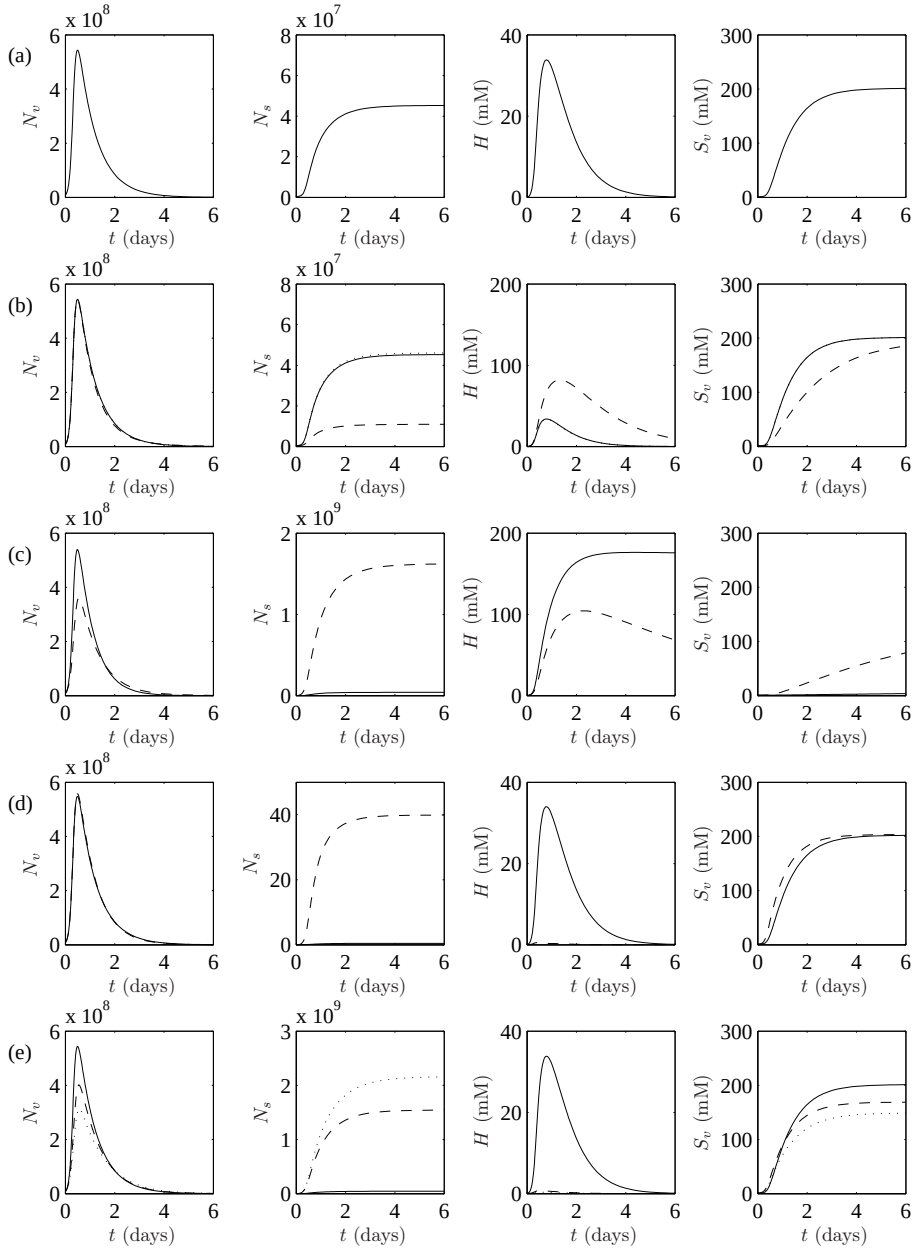

Figure A.13: Numerical solutions for the model whereby phosphorylated AgrA activates transcription of the putative kinase. (a) Wild-type solution ($\rho = 5 \times 10^{-8}, \xi = 5 \times 10^{-10}$). (b) Solid line: wild-type solution; dashed line: *agr* mutant; dotted line: *agr* mutant with $c_K = 0.2$ (indistinguishable from solid line for N_v, H and S_v). (c) Default parameters except $\rho = 5 \times 10^{-11}$. Solid line: $c_K = 0.1$ (default); dashed line: $c_K = 20$. (d) Default parameters except $\xi = 5 \times 10^{-18}$. Solid line: $c_K = 0.1$ (default); dashed line: $c_K = 10^6$. (e) Wild-type solution. Solid line: $c_K = 0.1$; dashed line: $c_K = 10$; dotted line: $c_K = 1000$.

AgrA∼P target	ρ	ξ
Transcription of *spo0A*	2×10^{-7}	2×10^{-9}
Transcription of the putative-kinase-associated gene	5×10^{-8}	5×10^{-10}
Transcription of the putative-phosphatase-associated gene	5×10^{-8}	6×10^{-10}
Phosphorylation of Spo0A	2×10^{-8}	2×10^{-10}

Table A.4: The values of ρ and ξ which are required to enable each model to reproduce wild-type-like behaviour.

Phosphorylated AgrA inhibits transcription of the putative phosphatase

The final case which we consider is AgrA∼P inhibiting transcription of the phosphatase which acts upon Spo0A∼P, i.e. increased cell density should prevent deactivation of Spo0A, thus enhancing the possibility that Spo0A induces sporulation and solventogenesis. In this scenario the equations for Spo0A, Spo0A∼P, AgrA and AgrA∼P are as for the preceding model (i.e. equations (A.5), (A.2), (A.3) and (A.4) respectively). The only other equation which we must alter from those described in the main paper is that for the putative phosphatase (in its unphosphorylated form). Thus (9) is replaced by

$$\frac{dP_h}{dt} = \frac{c_{P_h} U_{A^P}^{P_h}}{B_{A^P}^{P_h} A^P + U_{A^P}^{P_h}} - \phi_{S_A^P}^{P_h} P_h S_A^P + \psi_{P_h^P} P_h^P - (r(1 - N_v/\kappa) + \lambda_{P_h}) P_h. \tag{A.7}$$

Numerical solutions for this model are displayed in Figure A.14.

Appendix B. Alternative parameter choices

There are three parameters which we have identified in §2.5 as being worthy of further investigation since they were not guided by data or the literature; these are c_{agr}^{CA} (the constitutive production rate of AgrA and AgrC), μ_{agr} (the rate at which AgrB, AgrC and AgrD enter the cell membrane) and, finally, k_{agr} (the AIP production rate). All of these are associated with the 'strength' of the *agr* system and we expect that lowering the value of each will reduce the effect of the *agr* system, presumably resulting in less pronounced phenotypes. In Figures B.15–B.17 we see that this is indeed the case if AgrA∼P can donate its phosphate to Spo0A: reducing the values of each of these parameters below the default choice produces a lower spore count and solventogenesis occurs on a slower timescale. In addition, taking sufficiently small values of each of these parameters leads to each response being switched off, i.e. the *agr* system is rendered ineffective and kinase production (under the default parameter set) is not strong enough to reinstate the responses. Alterations to ρ (the rate of acid to solvent conversion) or ξ (the rate of spore formation) can restore the dynamics of the model to wild-type behaviour, neatly demonstrating the inter-dependence of

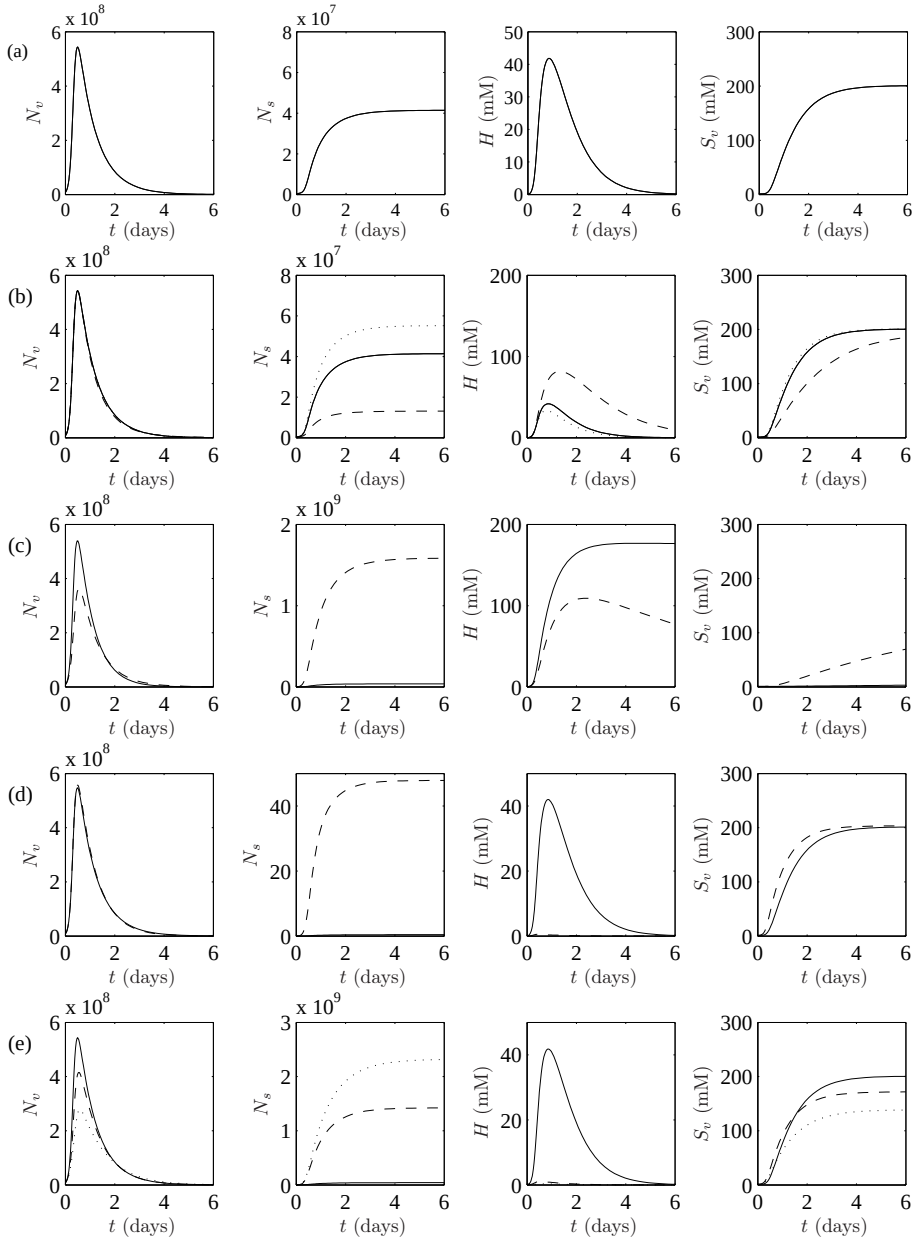

Figure A.14: Numerical solutions for the model whereby phosphorylated AgrA inhibits transcription of the putative phosphatase. (a) Wild-type solution ($\rho = 5 \times 10^{-8}, \xi = 6 \times 10^{-10}$). (b) Solid line: wild-type solution; dashed line: *agr* mutant, $c_K = 0.1$ (default); dotted line: *agr* mutant with $c_K = 0.2$. (c) Default parameters except $\rho = 5 \times 10^{-11}$. Solid line: $c_K = 0.1$ (default); dashed line: $c_K = 20$. (d) Default parameters except $\xi = 6 \times 10^{-18}$. Solid line: $c_K = 0.1$ (default); dashed line: $c_K = 10^6$. (e) Wild-type solution. Solid line: $c_K = 0.1$ (default); dashed line: $c_K = 10$; dotted line: $c_K = 1000$.

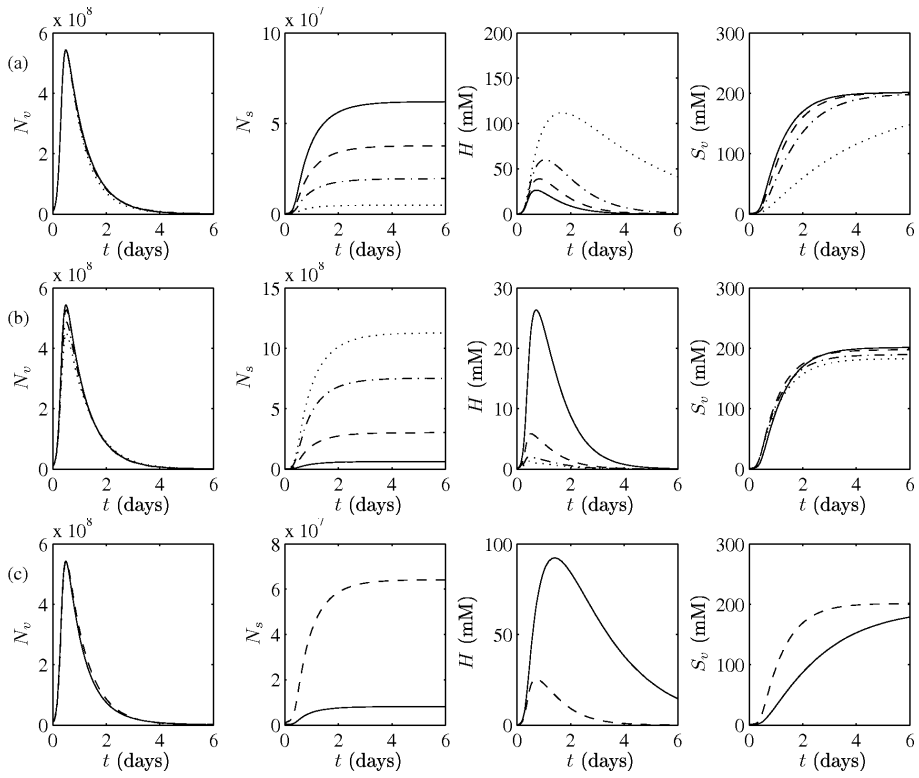

Figure B.15: (a) Numerical solution to equations (1)–(21) using the default parameter set displayed in Table 3 for all parameters except c_{agr}^{CA} for which we use solid line: $c_{agr}^{CA} = 4$ (the default value); dashed line: $c_{agr}^{CA} = 3$; dot-dash line: $c_{agr}^{CA} = 2$; dotted line: $c_{agr}^{CA} = 0.4$. Decreasing this parameter from its default value reduces the number of spores which can be formed and the speed at which solventogenesis occurs. For sufficiently small c_{agr}^{CA} both of these phenotypes can be suppressed. (b) As above with solid line: $c_{agr}^{CA} = 4$; dashed line: $c_{agr}^{CA} = 10$; dot-dash line: $c_{agr}^{CA} = 20$; dotted line $c_{agr}^{CA} = 40$. Increasing this parameter from its default value results in more spores and acid conversion taking place on a much faster timescale. (c) As above with $c_{agr}^{CA} = 1$ and solid line: ρ and ξ taken from the default parameter set; dashed line: $\rho = 1.5 \times 10^{-7}$ and $\xi = 1.5 \times 10^{-9}$. Altering ρ and ξ compensates for the reduction in c_{agr}^{CA} and enables wild-type-like behaviour to be restored.

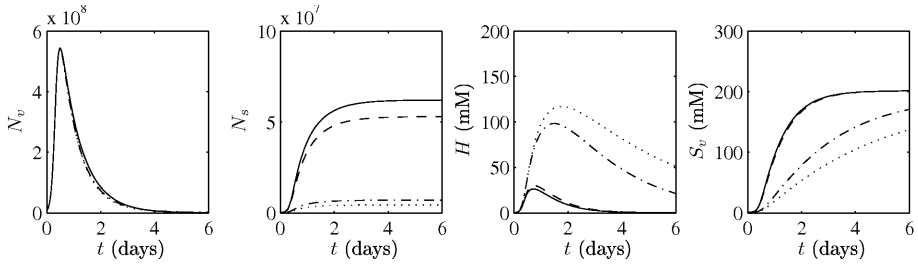

Figure B.16: Numerical solution to equations (1)–(21) using the default parameter set displayed in Table 3 for all parameters except μ_{agr} for which we take solid line: $\mu_{agr} = 1$ (the default value); dashed line: $\mu_{agr} = 10^{-2}$; dot-dash line: $\mu_{agr} = 10^{-4}$; dotted line: $\mu_{agr} = 10^{-5}$. Decreasing μ_{agr} is equivalent to reducing the rate at which the Agr proteins can enter the cell membrane (and thus reducing the rate at which they can become active) and this has a negative effect upon both sporulation and solventogenesis (illustrating that the *agr* system can be responsible for both of these phenotypes occurring). Increasing μ_{agr} from its default value ($\mu_{agr} = 1$), on the other hand, has negligible effect upon the system, suggesting that the *agr* system is functioning at its maximum capacity with this default value.

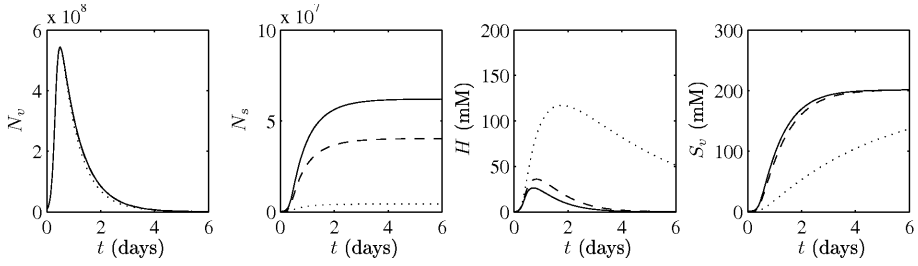

Figure B.17: Numerical solution to equations (1)–(21) using the default parameter set displayed in Table 3 for all parameters except k_{agr} for which we take solid line: $k_{agr} = 0.4$; dashed line: $k_{agr} = 10^{-8}$ and, finally, dotted line: $k_{agr} = 10^{-9}$. k_{agr} represents the rate of production of AIP (the signal molecule of the *agr* system whose density should correlate with population density). The results are qualitatively equivalent to those discussed for μ_{agr} in Figure B.16.

the parameters (to maintain wild-type-like responses from the model, if we increase the 'strength' of the *agr* system, ρ and ξ must be lowered, and vice versa). Furthermore, when different values of c_{agr}^{CA}, μ_{agr} and k_{agr} are used, equivalent qualitative results to those derived in §3.1 still can be achieved with regards to splitting the two phenotypes through alterations to ρ and ξ (data omitted for brevity).

In all of our simulations, the population density attains a high enough level to ensure that the *agr* system is up-regulated and therefore active. Thus, increasing c_{agr}^{CA} makes the behaviour of the clostridial *agr* system approach that of *S. aureus* (production rates of AgrA and AgrC become of a similar order to those of the staphylococcal *agr* system). Increasing μ_{agr} or k_{agr}, on the other hand, has negligible effect upon the system (we do not illustrate these in Figures B.16 and B.17 as the resulting numerical simulations are indistinguishable from the default wild-type solution), leaving c_{agr}^{CA} as a principal factor affecting sporulation and solventogenesis.

The above results pertain to the scenario in which AgrA∼P phosphorylates Spo0A. The remaining three networks, in general, appear to be more robust to alterations in these parameters (data not shown for brevity). Fewer spores are formed and solventogenesis slows down if c_{agr}^{CA}, k_{agr} or μ_{agr} are lowered when AgrA∼P affects transcription of the kinase and if c_{agr}^{CA} or k_{agr} are lowered when AgrA∼P affects transcription of the phosphatase. Otherwise, alterations to these parameters have little significant effect.

References

[1] Jones D.T., Woods D.R., Acetone-butanol fermentation revisited, Microbiol. Rev. 50 (1986) 484–524.

[2] Dürre P., Fischer R.J., Kuhn A., Lorenz K., Schreiber W., Stürzenhofecker B., Ullmann S., Winzer K., Sauer U., Solventogenic enzymes of *Clostridium acetobutylicum*: catalytic properties, genetic organization, and transcriptional regulation, FEMS Microbiol. Rev. 17 (1995) 251–262.

[3] Eichenberger P., Fujita M., Jensen S.T., Conlon E.M., Rudner D.Z., Wang S.T., Ferguson C., Haga K., Sato T., Liu J.S., Losick R., The program of gene transcription for a single differentiating cell type during sporulation in *Bacillus subtilis*, PLoS Biol. 2 (2004) 1664–1683.

[4] Piggot P.J., Coote J.G., Genetic aspects of bacterial endospore formation, Bacteriol. Rev. 40 (1976) 908–962.

[5] Piggot P.J., Hilbert D.W., Sporulation of *Bacillus subtilis*, Curr. Opin. Microbiol. 7 (2004) 579–586.

[6] Wilson M., McNab R., Henderson B., Bacterial disease mechanisms, an introduction to cellular microbiology, Cambridge University Press, 2002.

[7] Burbulys D., Trach K.A., Hoch J.A., Initiation of sporulation in *Bacillus subtilis* is controlled by a multicomponent phosphorelay, Cell 64 (1991) 545–552.

[8] Paredes C.J., Alsaker K.V., Papoutsakis E.T., A comparative genomic view of clostridial sporulation and physiology, Nature Rev. Microbiol. 3 (2005) 969–978.

[9] Jabbari S., Heap J.T., King J.R., Mathematical modelling of the sporulation initiation network in *Bacillus subtilis* revealing the dual role of the putative quorum-sensing signal molecule PhrA, Bull. Math. Biol. 73 (2011) 181–211.

[10] Hoch J.A., Regulation of the phosphorelay and the initiation of sporulation in *Bacillus subtilis*, Annu. Rev. Microbiol. 47 (1993) 441–465.

[11] Nölling J., Breton G., Omelchenko M.V., *et al.*, Genome sequence and comparative analysis of the solvent-producing bacterium *Clostridium acetobutylicum*, J. Bacteriol. 183 (2001) 4823–4838.

[12] Ravagnani A., Jennert K.C.B., Steiner E., Grünberg R., Jefferies J.R., Wilkinson S.R., Young D.I., Tidswell E.C., Brown D.P., Youngman P., Morris J.G., Young M., Spo0A directly controls the switch from acid to solvent production in solvent-forming clostridia, Mol. Microbiol. 37 (2000) 1172–1185.

[13] Harris L.M., Welker N.E., Papoutsakis E.T., Northern, morphological, and fermentation analysis of *spo0A* inactivation and overexpression in *Clostridium acetobutylicum* ATCC 824, J. Bacteriol. 184 (2002) 3586–3597.

[14] Steiner E., Scott J., Minton N.P., Winzer K., An *agr* quorum sensing system that regulates granulose formation and sporulation in *Clostridium acetobutylicum*, Appl. Environ. Microbiol. 78 (2012) 1113–1122.

[15] Novick R.P., Autoinduction and signal transduction in the regulation of staphylococcal virulence, Mol. Microbiol. 48 (2003) 1429–1449.

[16] Jabbari S., King J.R., Koerber A.J., Williams P., Mathematical modelling of the *agr* operon in *Staphylococcus aureus*, J. Math. Biol. 61 (2010) 17–54.

[17] Alsaker K.V., Papoutsakis E.T., Transcriptional program of early sporulation and stationary-phase events in *Clostridium acetobutylicum*, J. Bacteriol. 187 (2005) 7103–7118.

[18] Gustafsson E., Nilsson P., Karlsson S., Arvidson S., Characterizing the dynamics of the quorum-sensing system in *Staphylococcus aureus*, J. Mol. Microbiol. Biotechnol. 8 (2004) 232–242.

[19] Jabbari S., King J.R., Williams P., A mathematical investigation of the effects of inhibitor therapy on three putative phosphorylation cascades governing the two-component system of the *agr* operon., Math. Biosci. 225 (2010) 115–131.

[20] Bischofs I.B., Hug J.A., Liu A.W., Wolf D.M., Arkin A.P., Complexity in bacterial cell-cell communication: quorum signal integration and subpoplation signaling in the *Bacillus subtilis* phosphorelay, P. Natl. Acad. Sci. USA 106 (2009) 6459–6464.

[21] Voigt C.A., Wolf D.M., Arkin A.P., The *Bacillus subtilis sin* operon: an evolvable network motif, Genetics 169 (2005) 1187–1202.

[22] Senger R.S., Papoutsakis E.T., Genome-scale model for Clostridium acetobutylicum: Part I. Metabolic network resolution and analysis, Biotechnol. Bioeng. 101 (2008) 1036–1052.

[23] Senger R.S., Papoutsakis E.T., Genome-scale model for Clostridium acetobutylicum: Part II. Development of specific proton flux states and numerically determined sub-systems, Biotechnol. Bioeng. 101 (2008) 1053–1071.

[24] Shinto H., Tashiro Y., Yamashita M., Kobayashi G., Sekiguchi T., Hanai T., Kuriya Y., Okamoto M., Sonomoto K., Kinetic modeling and sensitivity analysis of acetone-butanol-ethanol production, J. Biotechnol. 131 (2007) 45–56.

[25] Votruba J., Volesky B., Yerushalmi L., Mathematical model of a batch acetone-butanol fermentation, Biotechnol. Bioeng. 28 (1986) 247–255.

[26] Haus S., Jabbari S., Millat T., Janssen H., Fischer R.J., Bahl H., King J.R., Wolkenhauer O., A systems biology study of the effect of pH-induced gene regulation on the metabolic network governing solvent production by *Clostridium acetobutylicum* in continuous culture, BMC Systems Biology 5 (2011) 10.

[27] Scotcher M.C., Rudolph F.B., Bennett G.N., Expression of *abrB310* and *sinR*, and effects of decreased *abrB310* expression on the transition from acidogenesis to solventogenesis, in *Clostridium acetobutylicum* ATCC 824, Appl. Environ. Microbiol. 71 (2005) 1987–1995.

[28] Steiner E., Dago A.E., Young D.I., Heap J.T., Minton N.P., Hoch J.A., Young M., Multiple orphan histidine kinases interact directly with Spo0A to control the initation of endospore formation in *Clostridium acetobutylicum*, Mol. Microbiol. 80 (2011) 641–654.

[29] Wörner K., Szurmant H., Chiang C., Hoch J.A., Phosphorylation and functional analysis of the sporulation initiation factor Spo0A from *Clostridium botulinum*, Mol. Microbiol. 59 (2006) 1000–1012.

[30] Wuster A., Babu M.M., Conservation and evolutionary dynamics of the *agr* cell-to-cell communication system across firmicutes, J. Bacteriol. 190 (2008) 743–746.

[31] Paredes C.J., Rigoutsos I., Papoutsakis E.T. , Transcriptional organization of the *Clostridium acetobutylicum* genome, Nucleic Acids Res. 32 (2004) 1973–1981.